Normal Yielding NY and Compression-induced Critical Stress Intensity Factor K_{IIcr}^{c}
- Missing Links in an Isotropic 'Closed' Macro-Mechanics Building –
→ *Does a generic number 2 for isotropic materials exist?*
Search on basis of Cuntze's Failure Mode Concept

1 Design Verification and Associated Essential Designations
2 Material Symmetry-based Assumed System of Quantities and Modes
3 Material Symmetry-dedicated Basis of Cuntze's Failure-Mode-Concept FMC
4 FMC Applications to Brittle Dense Concrete, Porous Material (foam)
5 FMC Application to Normal Yielding, NY (crazing, PMMA)
6 Existence of a critical Stress Intensity Factor under Compression K_{IIcr}^{c}
7 Conclusions & Outlook

1. Design Verification and Associated Essential Designations

1.1 General

Fig.1 displays the structural engineer's tasks he is involved when designing a structural part. It is to demonstrate that the static Dimensioning Load Cases as well as the dynamic ones, considering lifetime, are fulfilled. Addressed are Design Dimensioning (Auslegung, Bemessung) and Design Verification (Nachweis), respectively proof. Of special focus there is the strength verification of non-cracked as well as the fracture mechanics verification of cracked structural components.

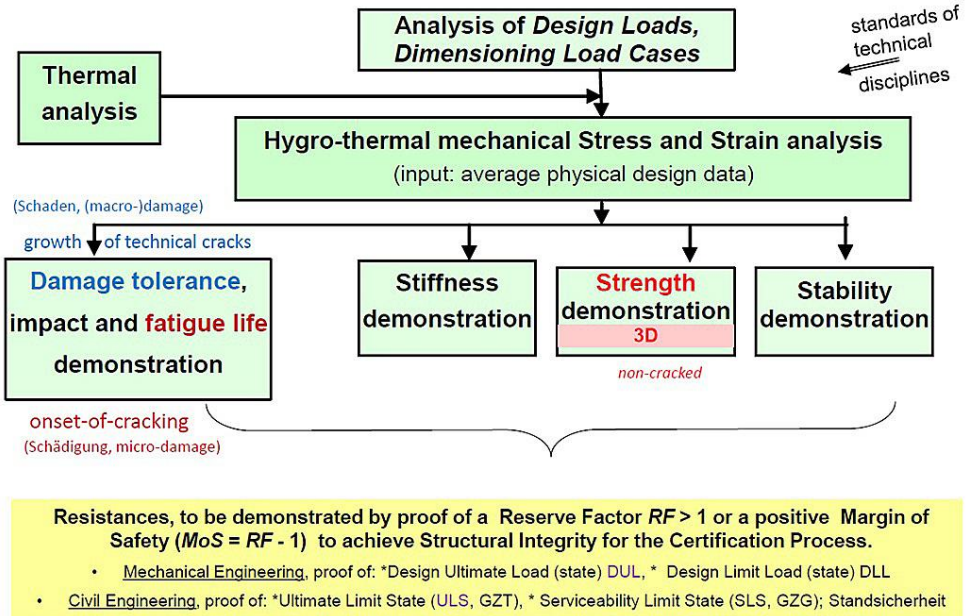

Fig.1: Structural engineer's tasks

Prof. Dr.-Ing. habil. Ralf Cuntze VDI, engineer and hobby material modeler
Ingenieurbüro für Leichtbau, Markt Indersdorf, Ralf_Cuntze@t-online.de, 0049 8136 7754
Retired from industry, linked to Composites United e. V., board member of CU Construction

Results of a long-lasting, time-consuming never funded "hobby"

The size of the (macro-)damage decides whether it is to apply a Strength Failure Condition SFC (now most often termed strength criterion) for the verification of onset-of-fracture of the un-cracked structural part or a Damage Tolerance Condition in case of a technical crack.

Fig.2 gives hints where which verification procedure is to apply or in other words: When must be fracture mechanics used and when strength mechanics?

The figure refers to: (a) Strength Mechanics versus Linear Elastic Fracture Mechanics (LEFM) analysis; (b) Crack-free and crack-driven fracture through a_0 being an initial flaw size (surface flaw, delamination) or a developed crack. *Fig.2* depicts where the different technical failure types Normal Fracture NF, Shear Fracture SF and Shear Yielding SY, Normal Yielding NY are located.

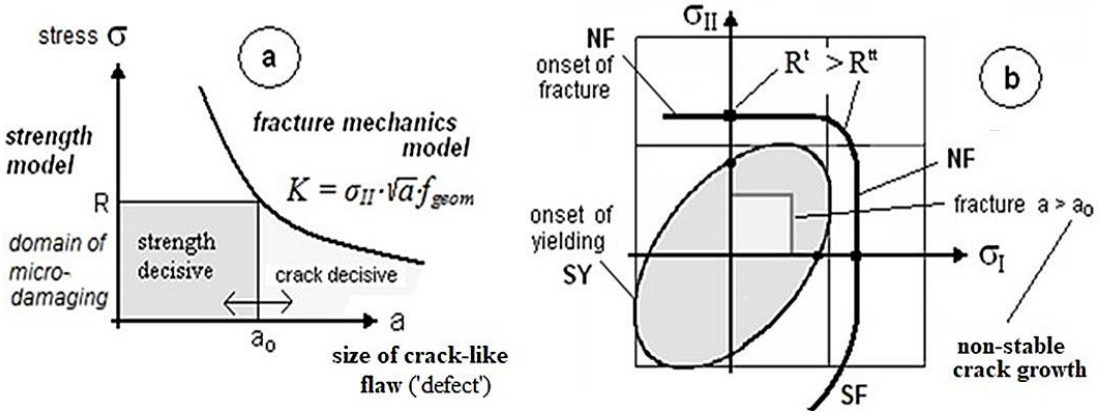

Fig.2: Strength mechanics versus fracture mechanics K is stress intensity factor, a is crack size, NF is Normal Fracture, SF is Shear Fracture, R is strength value, ^{t} is tensile

Design strength of a structural component is demonstrated:

"*If no relevant limit failure state is met* and *if all dimensioning load cases are considered"*.

Structural load-carrying capacity is mainly determined on material level by the stress situation in the critical material location. The grade of local stress singularity in the component is to consider.

For a general stress state the LEFM situation is fully similar to strength mechanics. Each mode contributes to the failures activated by the 3D-stress state:

* Strength Mechanics: If all strength failure modes are activated then the failure condition beyond which onset-of-failure will occur reads $Eff / Eff_{cr} = 1 = 100\%$ with $Eff = f(Eff^{modes})$

* Fracture Mechanics: If all fracture mechanics failure modes are activated then the failure condition beyond which the crack will begin to propagate reads $\mathcal{G} / \mathcal{G}_{cr} = 1$ with $\mathcal{G} = \mathcal{G}_I + \mathcal{G}_{II} + \mathcal{G}_{III}$ and $\mathcal{G}_{cr}$ the critical energy release rate.

1.2 Designations

For a better understanding, because many disciplines are met, some designations are presented:

Cohesive strength: maximum tensile stress σ^t (≡ separation strength R^t) of bonding between surfaces or particles building a material. However, in rock and soil mechanics differently defined as the inherent shear strength R^τ (≡ max τ_n) of a plane where the normal compressive stress $\sigma_n^c = 0$

Composite Material (Verbundwerkstoff): material made from constituent materials, that when combined, produce a material with characteristics different from the individual component (Fiber Reinforced Plastic, Concrete, Glare, Ceramic Matrix Composites, Fiber Metal Laminate etc.). Often, a Composite Material can be homogenized on the macro-mechanics level. This is advantageous because a homogenized material via its 'smeared' composite properties is relatively simple to model, analyze and test

Confining pressure: lithostatic pressure in geo-mechanics, the pressure forced on a layer of soil or rock by the heaviness of the overlying substance. Corresponds to a hydrostatic pressure p_{hyd}

Confining stress: usually stress σ_z caused by p_{hyd} at level z

Damage (Beschädigung): physical harm, which captures in English as well micro-damage (Schädigung) as macro-damage (Schaden)

Effective Stress: degraded material-related stress that considers a reduced load-carrying cross-section $\sigma_{ef} = \sigma / (1\text{-}D)$ with D the degradation sum

Equivalent stress σ_{eq}: (a) equivalent to the stress state, as performed in σ_{eq}^{Mises}, and (b) comparable to the value of the strength R which dominates one single failure mode or failure type

Failure: state of inability of an item to perform a required function in its limit state. A structural part does not fulfil its functional requirements such as the failure modes Onset-of-Yielding, brittle fracture (NF, SF, Crushing Fracture CrF), Fiber-Failure FF, Inter-Fiber-Failure IFF (matrix failure), leakage, deformation limit (tube widening), delamination size limit, frequency bound, or heat flow etc. A failure is a project-defined 'defect'. For each failure mode a Limit State with F = Limit State Function or Failure Function is to formulate. A specific failure example is: A 2nd loading, under a distinct failure mode (here SF), cannot be sustained anymore, like a slightly porous UltraHighPerformanceConcrete UHPC compression test specimen after a crushing test under p_{hyd} = 1000 MPa where the first loading of the crumbles might have been still further increased, densification enables it)

Failure Criterion: $F > = < 1$, Failure Condition: $F = 1 = 100\%$

Failure Mode: Failure mode is a commonly used generic term for the types of failures, is a name for a potential way a system may fail (in design verification usually a project- associated failure)

Failure Surface and Failure Body: the surface of the failure body is the shape defined by $F = 1$

Failure Type (isotropic): NF, SF, CrF, Normal Yielding NY, Shear Yielding SY

Flaw versus micro-crack: a micro-crack is a sharp flaw (Ungänze), grade of singularity is decisive

Flow curve: Stress–Strain Curve minus is elastic part (proportional)

Fracture: separation of a whole into parts

Fracture Toughness: ability to withstand crack growth (≡ critical Stress Intensity Factor SIF, K_c)

Friction: slope of the Mohr failure envelope defined as ratio of the shear stress τ_n to the normal stress at failure $max\ \sigma_n^c$. Ratio is termed internal friction value μ ('linear Mohr-Coulomb' is valid)

'Global' and 'Modal' SFC: 'global' shall describe the full failure surface by one single equation capturing all existing failure modes and 'modal' shall describe plain failure mode parts of the full failure surface by an associate failure mode equation SFC

Inelastic versus plastic: *inelastic* → micro-damage, brittle, fracture mod*es*, friction occurs and is indicated by the paraboloid-shaped SFCs (see later formulas), inelastic potential (not yield potential); *plastic* → metal plasticity, ductile, yield mod*e*, frictionless sliding indicated by the cylinder shape of 'Mises', yield potential

Material: 'homogenized' (macro-)model of the envisaged complex solid or heterogeneous material combination which principally may be a metal, a lamina or further a laminate stack analyzed with effective properties. Homogenizing (smearing) simplifies modelling

Material behavior: *brittle* behavior could be characterized with the complete loss of tensile strength capacity at first fracture, R^t. Quasi-brittle behavior shows - after reaching R^t - a slight strain hardening followed by a gradual decay of tensile strength capacity during a strain softening domain. *Ductile* behavior is accompanied by a gradual increase of tensile stress (strain hardening), and after reaching R^t a strain softening domain follows

Material Composite (Werkstoffverbund): Composite of different constituent materials, where structure-mechanically a composite construction is still given like for Carbon Concrete Composite (≠ composite material). Practically, the constituent materials of a material composite cannot be 'smeared' to a material

Material Stressing Effort (Werkstoffanstrengung): max*Eff* =100% is reached at $F = 1 = 100\%$

Splitting (longitudinal): failure mechanism, resulting from compression loading that creates cracks parallel to the compression load axis generated by perpendicular tensile stresses acting at internal flaw tips which are usually combined with wing cracks

Strength Failure Condition (SFC): mathematical formulation of the strength failure surface, that takes the form $F = 1$. Tool, to assess a 'multi-axial failure stress state' in a critical material location of the structural component. The SFC should consider, that failure usually occurs at a

lower than macro-mechanic level, micromechanically, such as the matrix in a the macro-mechanically described SFC of the composite material

Stress (not stress component): component of the stress tensor defined as force divided by the area of the cross-section

Stress intensity factor (SIF) K_c: measure of the intensity of the stress state in the vicinity of the crack tip, multifold of the so-called stress singularity $1/\sqrt{2\pi r}$

Stress –Strain Curve: curve capturing in compression domains and tensile domains the elastic, the strain-hardening (in construction often termed tension hardening) and the strain-softening (if applicable) curve parts. For mapping, engineers often use the Ramberg-Osgood function

Yield strength: As it is difficult to determine a precise onset-of-yield point, in general, one should discriminate from practical reasons the proportional (tensile) limit R_p ($\equiv f_v$) and $R_{p0.2}$ ($\equiv R_{0.2}^t$), where the offset yield point is taken as the stress at which 0.2% plastic deformation remains

120°-symmetry of the isotropic failure body: according to the equality of the 3 principal stresses each 'perturbation' of the rotational failure body exists 3 times

Strength denotations: R is strength, in general, and also the statistically-reduced value. $\bar{R}$ is average strength which is used when mapping a course of test data points. In construction: letter f.

2. Material Symmetry-based Assumed System of Quantities and Modes

2.1 General

In the development of structural components the application of 3D-validated strength failure conditions SFCs ('criteria') is one essential pre-condition for achieving the required fidelity for the user. This includes Yield Failure Conditions (ductile behavior) for the non-linear analysis of the material and the Onset-of-Yielding limit verification. And it further includes conditions to verify that fracture does not occur, i.e. for Onset-of-Fracture (brittle and ductile behavior). The Fracture Failure Conditions confine by $F = 1$ the load-driven growth of a existing 'friction-free' yield surface. Instead of the SFC formulation $F = 1$, equivalently, the so-called Material Stressing Effort (Werkstoffanstrengung) $Eff = 100\%$ can be used.

Since two decades the author believes in a macroscopically-phenomenological 'complete classification' system, where all strength failure types are included, see *Fig.3*. In his assumed system several relationships may be recognized: (1) shear stress yielding SY, followed by shear fracture SF viewing 'dense' materials. For porous materials under compression, the SF for dense materials is replaced by crushing fracture CrF. (2) However, to complete a system. What is with normal fracture NF? Is there a normal stress yielding NY corresponding to SY?

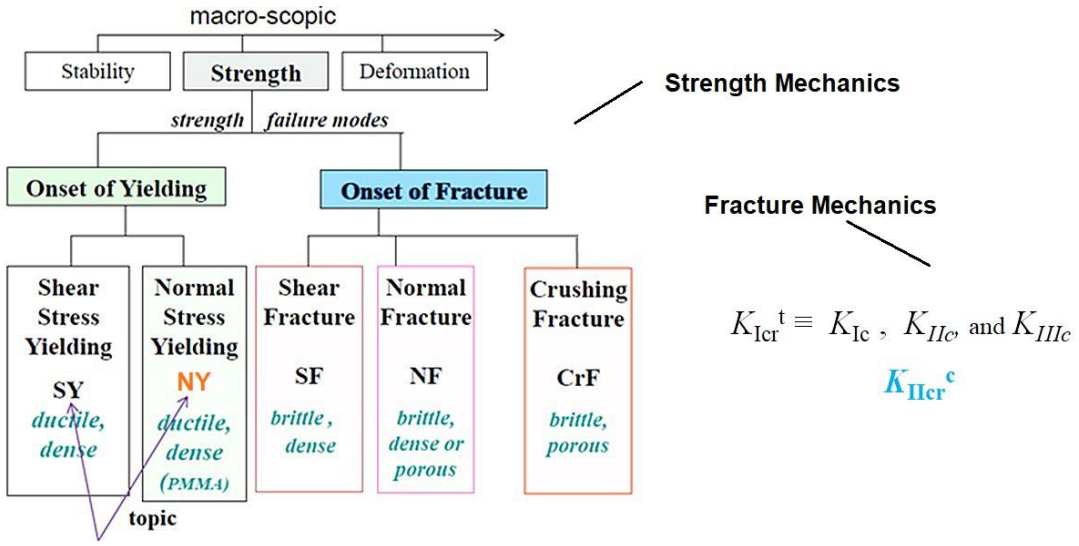

Fig.3: Assumed system of strength failure modes and the searched missing links NY, K_{IIcr}^{c}

Capturing all kinds of possible types of failure in a uniform classification is challenging, because the classification can be carried out according to different ways. The author thinks that a material behavior-overarching system delivers a good classification scheme for a 'macro-mechanics building of all materials'. This scheme should be clear and as simple as possible for the dimensioning structural engineer without violating any material-typical facts. In consequence, the author concludes: If one knows from a similar behaving material something about the behavior of the 'new' material, then pre-dimensioning with the new material becomes easier and more trusting.

According to the macroscopic load deformation curve, one can distinguish between deformation-poor and deformation-rich fracture processes. Here, too, the real material plays only a minor role. A mineral material can exhibit the same macroscopic behavior as a carbon fiber material, as a cast material or as a ferritic steel in the low-temperature range. And, a metal and a polymer can show large irreversible deformations up to fracture, although the micromechanical deformation mechanisms are different.

The micromechanical failure mechanisms of fracture are material-specific and therefore arbitrarily diverse. This is where (micro-)damage models come in. Some of what appears "similar" at the macro level (e.g. "brittle" behavior) may turn out to be completely different on the micro level. Examples are: A cleavage fracture in ferritic steels is for instance preceded by local *plastic deformations*. A fracture failure of concrete for instance implies small deformations from *damage mechanisms* on different length scales, micro-damage and macro-damage due to the complex microstructure,

Macroscopic fractures can be classified spanning deformation-rich and deformation-poor (grey casting, concrete) fractures, respectively. In tension and compression, the deformation-rich material experiences sliding failure under the influence of the failure-driving shear stress. In the deformation-poor case, the material is plastically non-deformable and breaks under tension perpendicular to the tensile stress as soon as the normal stress reaches the separation strength R^t or tensile strength, respectively. This is accompanied by cleavage fracture designated here as Normal Fracture NF.

Compression of brittle materials causes shear failure, because the shear stress is decisive. This includes as well sliding failure of ductile materials in the tensile and the compressive range as friction-sliding fracture failure of brittle materials in the compressive range.

2.2 Missing link 'Normal Yielding NY'

Is there Normal Yielding? NY is known for a long time, but not in structural mechanics. An explanation for the 'Not known' is that a describing yield failure condition F^{NY} was missing. For establishing this missing link in his 'complete system' the author found applicable test data which he evaluated and visualized in chapter 5.

2.3 Missing link 'Critical Stress Intensity Factor (SIF) under compression'

The other missing link, investigated in this paper, is a critical Stress Intensity Factor (SIF) or fracture toughness under a compression-induced shear, K_{IIcr}^{c}. This missing link will be presented by the author in chapter 6. *The author admits at this point that this SIF is not relevant for the treatment of common fracture-mechanical tasks in the tensile and compression range because it requires an ideal homogeneous crack-tip situation. However, he believes that the receipt of* K_{IIcr}^{c} *is an important theoretical task for achieving a 'complete system'.*

The author remembers a two decades old citation of A. Carpinteri that approximately read:" With homogeneous isotropic brittle materials there are 2 real energy release rates $\mathcal{G}_{Icr}$, $\mathcal{G}_{IIcr}$, one in tension and one in compression. These two $\mathcal{G}s = K^2 \cdot (1-\nu^2) / E$ (plane strain) possess the attribute that the crack plane does not turn and are therefore real (or 'basic') material properties."
This forced the author at that time to intensively search K_{IIcr}^{c} as the basic pendant to K_{Icr}^{t}, officially written $\boldsymbol{K_{Ic}}$. Later the author postulated in the sense of Carpinteri:

"***Only a stable crack growth plane-associated SIF is a 'basic' fracture mechanics property"***.

This is valid in the tension domain for the SIF K_{Ic} above and not for K_{IIc} and K_{IIIc}. It should be valid in the compression domain, too, that means shear, for a $\boldsymbol{K_{IIcr}^{c}}$.

3. Material Symmetry-dedicated Basics of Cuntze's Failure-Mode-Concept FMC

Helpful information is coming from demands of the material symmetry: A basic (fixed) number of material quantities can be derived from the corresponding tensors. This gives a minimum of 'generic' numbers, which is crucial for theoretical modeling and for the testing effort. For isotropic materials this generic number is 2. Hence, the author's full idea can be formulated as:

1 If a material element can be homogenized to an ideal crystal (= frictionless),
then, material symmetry demands for the Isotropic Material are:
- 2 e*lastic 'constants', 2 strengths,* ***2 fracture toughness values, 2 'basic' invariants* I_1, J_2*** and ***2 strength failure modes,*** for ***yielding*** two (NY, SY) and for ***fracture*** two (NF, SF)
(* for transversely-isotropic UD-materials, generic number 5, one also needs just 5 invariants for formulating SFCs. This is valid as long as a one-fold acting failure mode is to describe by the distinct SFC and not a multi-fold one)
- 1 *physical parameter (such as coefficient of thermal expansion CTE, coefficient of moisture expansion CME, material friction, etc.)*

(for UD- materials the witnessed respective numbers are 5 and 2 for physical parameters)

2 Mohr-Coulomb requires for the real crystal another inherent parameter,
- the *physical parameter 'inherent material friction' μ*

3 Fracture morphology gives finally evidence
- Each strength corresponds to a distinct *strength failure mode* and to a distinct *strength fracture type,* to Normal Fracture (NF) or Shear Fracture (SF)

4 Densely packed frictional material experiences dilatation when sheared.

From above follows an advantage when material symmetry knowledge is applied: Presuming, homogeneity is a valid assessment for the task-determined model, just a minimum number of properties must be measured, only. These are significant benefits in cost and time.

Considering all these similarities

"Why should the basic SIF $\boldsymbol{K_{IIcr}^{c}}$ or the NY mode not exist?"

3.1 Invariants and their application

Following the knowledge above, the FMC postulates in its approach:

Number of failure modes = number of strengths!

Material symmetry demands give reason that the FMC just strictly describes single independent failure modes by its failure mode–wise concept. This will make the derivation of equivalent stresses possible. In parallel to the material symmetry demands and the strict failure-mode thinking, further driving ideas were using invariants and considering their physical content, *Fig.4*.

$$I_1 = (\sigma_I + \sigma_{II} + \sigma_{III}) \;=\; f(\sigma)\;,\quad 6J_2 = (\sigma_I - \sigma_{II})^2 + (\sigma_{II} - \sigma_{III})^2 + (\sigma_{III} - \sigma_I)^2 = \; f(\tau)$$ 'Mises' invariant

$$27J_3 = \; (2\sigma_I - \sigma_{II} - \sigma_{III}) \cdot (2\sigma_{II} - \sigma_I - \sigma_{III}) \cdot (2\sigma_{III} - \sigma_I - \sigma_{II}),$$

$$3 \cdot \sigma_{oct} = \sigma_I + \sigma_{II} + \sigma_{III} = \; \sigma_\ell + \sigma_n + \sigma_t \;\; ; \;\; 9 \cdot \tau_{oct}{}^2 = 6J_2 = 4 \cdot (\tau_{III}{}^2 + \tau_I{}^2 + \tau_{II}{}^2),\;\; \tau_{II} = \max \tau (mathem.)$$

$\sigma_I, \sigma_{II}, \sigma_{III}$ are principal stresses, $\sigma_I > \sigma_{II} > \sigma_{III}$ are mathematical stresses (> means more positive)

shape change friction volume change

$$F^{SF} = \; c_1^{SF} \cdot \frac{3J_2 \cdot \Theta^{SF}}{(\bar{R}^c)^2} \;+\; c_2^{SF}(\mu) \cdot \frac{I_1}{\bar{R}^c} \;+\; c_3^{SF} \cdot (\frac{I_1}{\bar{R}^c})^2 \;=\; 1$$

'Mises Cylinder'

(Above *general* strength failure condition SFC is normalized by the compressive strength)

Two-fold failure danger can be modelled by using the well known invariant J_3.

The non-circularity function Θ^{SF} includes d^{SF} as non-circularity parameter.

It represents the 120°symmetry of isotropic materials, caused by the equivalency of the 3 principal stresses and directions (see the following fracture bodies).

$$\Theta^{SF}(J_3) = \sqrt[3]{1 + d^{SF} \cdot \sin(3\vartheta)} = \sqrt[3]{1 + d^{SF} \cdot 1.5 \cdot \sqrt{3} \cdot J_3 \cdot J_2{}^{-1.5}}$$

Fig.4: Schematic example for the use of invariants for isotropic, slightly porous materials, $I_1 < 0$

In this context the Hypothesis of Beltrami states: *"At onset-of-yielding, the strain energy density W in a material element consists of two portions; one describing the strain energy due to a change in volume (dilatation, dilation in US) and another strain energy proportion due to a change in shape (distortion)"*. These two portions can be related to invariants: The dilatational energy to I_1^2 for a volume change and the distortional energy to $J_2 \equiv$ ('Mises') for a shear distortion under volume consistency, forming a shape change of the material element. If friction is activated under compression then the frictional energy is to consider applying I_1. In *Fig.4* this dedication of invariants is exemplarily applied.

Lessons Learned (US), LL by the author: A brittle slightly porous concrete in the compression domain (p_{hyd}) can be SFC-described by the same SFC formula as a metal in the ductile rupture or 'Gurson tension domain', respectively due to similarly describable effects of the material element.

3.2 Two basic invariants are needed for generating strength failure conditions (stress criteria)

Following the contents of the previous sub-chapters for the derivation of invariant-based SFCs just two invariants are necessary to describe a failure mode.

J_3 is required when the same 'strength fracture mode' multiply occurs, which practically means for brittle isotropic materials that a 120° rotational symmetry of the fracture body is to face. The author was able to use these material symmetry specifications successfully in strength mechanics, using his failure mode concept for homogenized isotropic and for UD materials in many data sets.

In this context different effects are to discuss:

Mixed Strength (fracture) Failure: Different failure modes may be activated by the acting stress state. The interaction of both the activated fracture mode types Normal Fracture NF with Shear Fracture SF under compression increases the danger to fail! Hence, the associated fracture test data are so-called joint-probabilistic results of 2 modes!

Multi-fold (fracture) Failure Mode: The acting stress state with maximally equal orthogonal stresses activates the same mode multi-fold. Hence, the associated fracture test data are so-called joint-probabilistic results of a multi-fold acting mode!

A multi-fold occurrence is additionally to consider in the SFC formulas, using here J_3

(Example isotropic material: $\sigma_I = \sigma_{II}$, $\sigma_I = \sigma_{II} = \sigma_{III} \rightarrow \sigma_{hyd}$; 3-fold)

A multi-fold fracture mode increases the danger to fail ! $R^t > R^{tt}$ *(weakest-link effect),* $I_1 > 0$

A multi-fold failure mode decreases danger to craze ! $R^{tt} > R^t$ *(weakest-link effect),* $I_1 > 0$ (**NY**)

A multi-fold fracture mode increases the danger to fail ! $R^c > R^{cc}$ *(weakest-link effect),* $I_1 < 0$*, porous*

A multi-fold fracture mode decreases the danger to fail ! $R^{cc} > R^c$ *(redundancy effect),* $I_1 < 0$*, dense*

Bi-axial compression may further activate a critical tensile strain, which must be checked.

Physics-based SFC – usually – consider just one single failure mechanism and do not capture the bi-axial effect of $\sigma_I = \sigma_{II}$ or hydrostatic tensile or compressive failure stress states. This must be considered by an additional term!

The case, *2-fold* or $\sigma_{II} = \sigma_I$, is the reason for the 120°-symmetry of isotropic brittle behaving materials in the domains $I_1 > 0$ and < 0. This causes inward and outward dents and is elegantly solved by applying the invariant J_3 in the π-plane (hoop or deviatoric plane). The dents may be seen and modelled as pertubations on the surface of the failure body (Whether this additional modelling is necessary could not cleared by the author).

The case *3-fold with* $\sigma_{II} = \sigma_I = \sigma_{III}$, termed hydrostatic stressing, is solved with a closing tensile cap if failure occurs under this stress state and with a closing bottom under a compressive stress state in the case of porous materials.

LL: (1) Three energy terms – represented by two invariants, only - are required to establish SFCs; (2) Usual SFCs just describe a failure situation where a failure type occurs one-fold; (3) SFCs, that describe multi-fold failure situations and thereby regarding inward and outward dents of the failure body, require the third invariant J_3.

3.2 'Global' and 'Modal' strength failure conditions

Basically, there are two types of brittle Strength Failure Conditions SFCs employed, see *Fig.5*. The author gave them self-explaining names. The global SFC spans all strength failure modes whereas the modal SFC describes just a single SFC.
Here, global and modal have the same level of abstraction, as in the case of stability.
In order to only use experimentally derivable material quantities, the author directly introduced in his 3D-SFCs for the compression domain, internal friction μ as a formula parameter. Friction is a well-known physical property in engineering. One does not yet find a direct use of μ in the textbooks! Why using Mohr's friction angle φ if μ *(*φ*)* exists?

LL: (1) It is advantageous from physical and from modelling reasons not to employ 'global' SFCs. (2) A direct use of the friction value μ matches with engineer's thinking.

3.3 Basic features of the Failure-Mode-Concept FMC (formulated in 1995)

- Each failure mode represents 1 independent failure mechanism, and thereby represents 1 piece of the complete (global) failure surface
- Each failure mechanism is governed by 1 basic strength (this is witnessed)
- Each failure mode can be represented by 1 failure condition SFC. Therefore, equivalent stresses can be computed for each mode. This is of further advantage when deriving S-N curves and Haigh diagrams with minimum test effort

• Consequently, the FMC-approach requires the interaction of all (isotropic 2) modes!

$$Eff = \sqrt[m]{(Eff^{\text{mode 1}})^m + (Eff^{\text{mode 2}})^m + ...} = 1 = 100\%, \; if \quad \text{Onset of Failure}$$

From engineering reasons, Cuntze takes the same interaction exponent *m* for each transition domain between failure mode domains. The interaction of adjacent failure modes is modelled with the 'series failure system". That permits to formulate the total material stressing effort from all activated failure modes = 'accumulation' of Effs ≡ sum of all the failure danger proportions.

Eff = 1 represents the mathematical description of the failure body

• The value of the interaction exponent *m* depends on the ratio R^c/R^t. For brittle materials with about $R^c/R^t > 3$ the value is about *m* = 2.6. A smaller *m* is on the safe side. For slightly brittle materials R^c/R^t is about 5 and more from mapping experience in the transition zone of the two modes.

LL: The use of the entity Eff excellently supports 'understanding the multi-axial strength capacity of materials'.

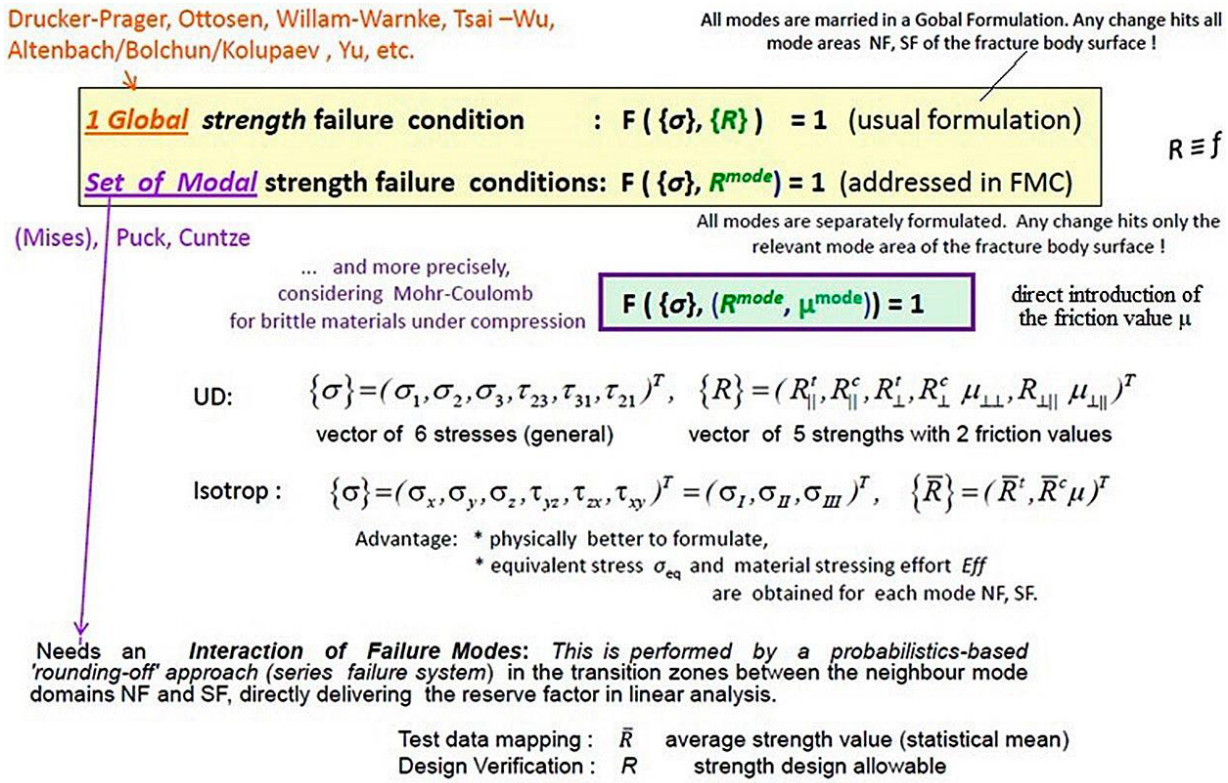

Fig.5: Scheme of 'global' and 'modal' strength failure conditions (f = strength in construction)

LL: The challenge is not the establishment of a SFC but the test data–based visualization of its associated fracture failure body, its failure curve in the principal stress plane as the bias cross-section of the body. And further, the different meridian curves as the axial cross-sections of the failure body with inward and outward dents along the 120°-symmetric isotropic failure body.

3.3 Basic features of the Failure-Mode-Concept FMC (formulated in 1995)

• Each failure mode represents 1 independent failure mechanism,
and thereby represents 1 piece of the complete (global) failure surface

• Each failure mechanism is governed by 1 basic strength (this is witnessed)

- Each failure mode can be represented by 1 failure condition SFC.
  Therefore, equivalent stresses can be computed for each mode. This is of further advantage when deriving S-N curves and Haigh diagrams with minimum test effort
- Consequently, the FMC-approach requires the interaction of all (isotropic 2) modes!

$$Eff = \sqrt[m]{(Eff^{\text{mode 1}})^m + (Eff^{\text{mode 2}})^m + ...} = 1 = 100\%, \; if \quad \text{Onset of Failure}$$

From engineering reasons, Cuntze takes the same interaction exponent *m* for each transition domain between failure mode domains. The interaction of adjacent failure modes is modelled with the 'series failure system". That permits to formulate the total material stressing effort from all activated failure modes = 'accumulation' of Effs ≡ sum of all the failure danger proportions.

Eff = 1 represents the mathematical description of the failure body

- The value of the interaction exponent *m* depends on the ratio R^c/R^t. For brittle materials with about $R^c/R^t > 3$ the value is about *m* = 2.6. A smaller *m* is on the safe side. For slightly brittle materials R^c/R^t is about 5 and more from mapping experience in the transition zone of the two modes.

LL: The use of the entity Eff excellently supports 'understanding the multi-axial strength capacity of materials'.

3.4 Visualization of a failure body

The fracture body is rendered here using the Haigh-Westergaard-Lode coordinates with $I_1/\sqrt{3}$ as y-coordinate and $\sqrt{2 \cdot J_2}$ as x-coordinate.

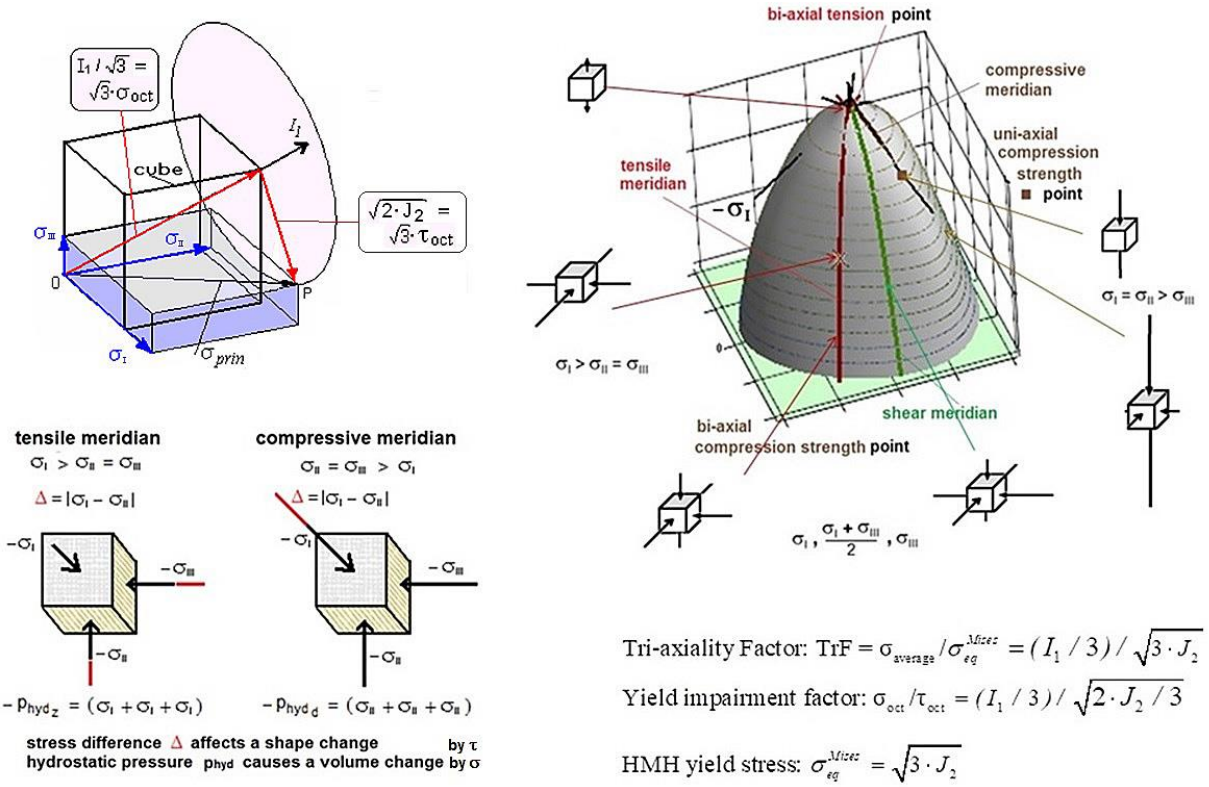

Fig.6: Visualization of the main meridians using Haigh-Westergaard Lode-coordinates $I_1/\sqrt{3}$, $\sqrt{2 \cdot J_2}$ and various multi-axial stress states. Squares ■ ■ indicate strength values and crosses bi-axial points

In *Fig.6* the upper left part figure confirms, that this coordinate choice physically makes sense.
The part figure left down, depicts the stress states belonging to a tensile meridian and to a compressive meridian, those axial cross–sections of the failure body (right) along on which most of the compression tests are run.
On the failure body outlined are the 3 main meridians including the shear meridian where the so-called Lode angle is zero due to the here chosen origin. For the tensile meridian it is +30° and for the compressive meridian -30°. 3D-stress states are added linked to the indicated failure body points.
Finally, for three essential design quantities the formulas are presented at the right side.

4. FMC-Applications to Brittle Dense Concretes and a Porous Foam

The following chapters show applications where 2D- and 3D-test data sets could be obtained by the author. For providing the sets to the author he is very grateful.
The two chapters 4.1 (Ultra-High-Performance-Concrete) and 4.2 (foam Rohacell) are incorporated to show the difference of plexiglass PMMA, chapter 4.3, to other materials in the quadrant I of the principal stress plane and to support the 'generic number 2' idea.

LL: A real validation of SFCs is with 3D test data only possible.

4.1 Onset of Fracture of isotropic, brittle, dense materials

As first application, demonstrating the versatility of the FMC-based SFCs, 3D test data of Ultra-High-Performance-Concrete UHPC from Dr. Speck, IfM (Prof. M. Curbach), TU-Dresden was mapped. Of main interest are the 2 meridians with its associated test data. These had to be extracted from the bulk of data by the author. *Fig.7* presents the provided test data.

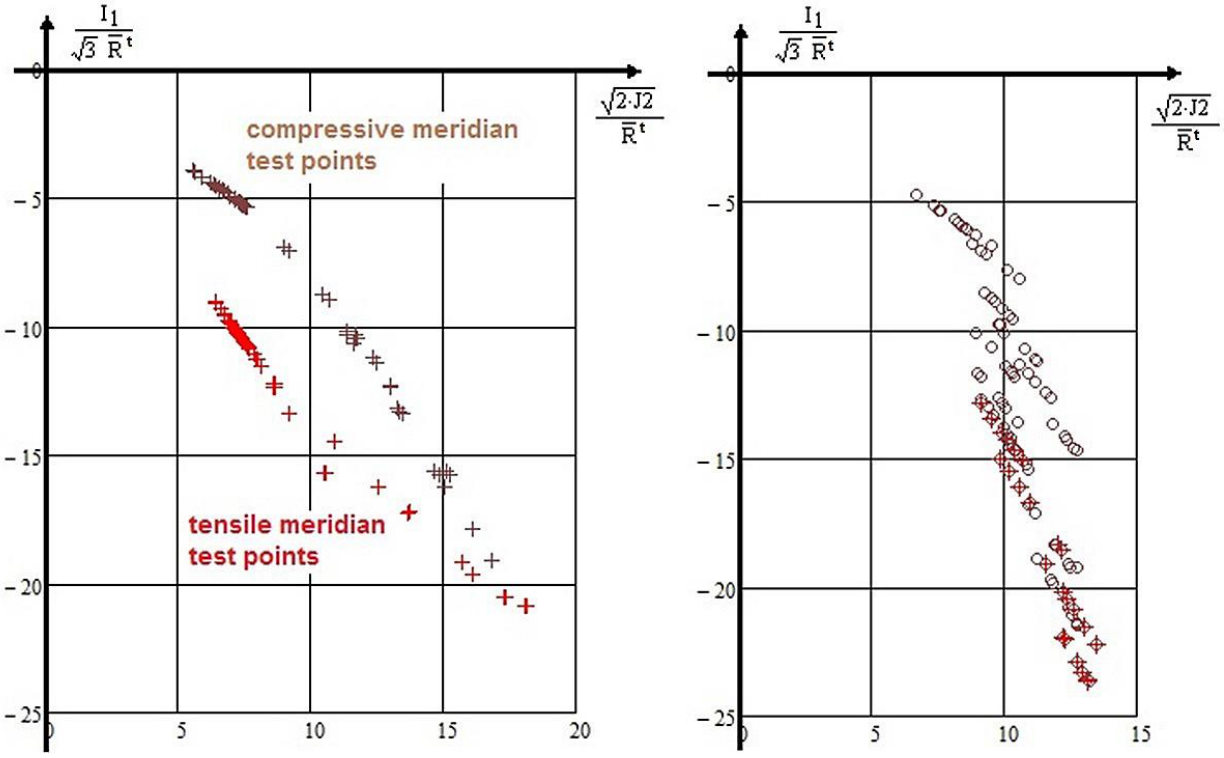

Fig.7: UHPC, (left) test points on the compressive (-30°) and the tensile meridian (+30°), extracted by the author; (right) full 3D-test data set. + test points on the meridians (real distance to the axis); o test points somewhere on the associated hoop ring

The FMC-based SFCs, applied in tensile and in compression domain, are presented in the *Table 1*

Table 1: SFC Formulas for NF and SF

Normal Fracture	**Shear Fracture**
$F^{NF} = c^{NF}(\Theta^{NF}) \cdot \frac{\sqrt{4J_2 \cdot \Theta^{NF} - I_1^2/3} + I_1}{2 \cdot \bar{R}_t} = 1$	$F^{SF} = c_1^{SF} \cdot \frac{3J_2 \cdot \Theta^{SF}}{\bar{R}^{c2}} + c_2^{SF} \cdot \frac{I_1}{\bar{R}^c} = 1$
$Eff^{NF} = c^{NF} \cdot \frac{\sqrt{4J_2 \cdot \Theta^{NF} - I_1^2/3} + I_1}{2 \cdot \bar{R}^t} = \sigma_{eq}^{NF} / \bar{R}^t$,	$Eff^{SF} = \frac{c_1^{SF} \cdot I_1 + \sqrt{(c_2^{SF} \cdot I_1)^2 + 12 \cdot c_1^{SF} \cdot 3J_2 \cdot (\Theta^{SF})}}{2 \cdot \bar{R}^c} = \sigma_{eq}^{SF} / \bar{R}^c$

Two-fold failure danger can be modelled by using the well known invariant J_3 including d = non-circularity parameter

$\Theta^{NF} = \sqrt[3]{1 + d^{NF} \cdot \sin(3\vartheta)} = \sqrt[3]{1 + d^{NF} \cdot 1.5 \cdot \sqrt{3} \cdot J_3 \cdot J_2^{-1.5}}$ *and* $\Theta^{SF} = \sqrt[3]{1 + d^{SF} \cdot \sin(3\vartheta)} = \sqrt[3]{1 + d^{SF} \cdot 1.5 \cdot \sqrt{3} \cdot J_3 \cdot J_2^{-1.5}}$

Lode angle ϑ , here set as $\sin(3 \cdot \vartheta)$ with 'neutral'shear meridian angle 0°; tensile meridian angle 30°; compr. m. a. -30°

A yield body is rotational symmetric , then $\Theta = 1$

A two-fold acting mode makes the rotational symmetric fracture body 120°-symmetric and is captured by $\Theta(J_3)$

Equation of the fracture body: $Eff = [(Eff^{NF})^m + (Eff^{SF})^m]^{m^{-1}} = 1 = 100\%$ *total effort*

$c_2^{SF} = (1 + 3 \cdot \mu)/(1 - 3 \cdot \mu)$, $\mu = \cos(2 \cdot \theta_{fp}^c \circ \cdot \pi / 180)$,

from fracture plane angle $\theta_{fp}^c \circ : 45°$ ($\mu = 0$), $50°$ ($\mu = 0.174$)

c^{NF}, Θ^{NF} from the two points ($\bar{R}^t$, 0, 0) and ($\bar{R}^{tt}$, $\bar{R}^{tt}$, 0) or by a minimum error fit, if data is available, and c^{CF}, Θ^{SF} from the two points (-$\bar{R}^c$, 0,0) and (-$\bar{R}^{cc}$, -$\bar{R}^{cc}$, 0) or by a minimum error fit
The failure surface is closed at the upper end: The closing cap shape is assumed on the safe side.

Notes: (1)The chosen NF-function enables to map a straight line of test data in the principle stress plane. (2) If the failure body is fully rotational symmetric then c^{NF} (Θ^{NF}=1 or d^{NF}=0) = 1. (3) Above NF can manage inward and outward dents by c^{NF} (Θ^{NF}) < 1 which renders the 120°-symmetry

Fig.8 displays the fracture failure body of the UHPC. Remarkable is the pretty triangle-shaped cross-section inherent to brittle isotropic materials. It depicts an outstanding 120°-symmetry, which is linked to the ratio of R^t / R^{tt}.

On the UHPC fracture body the uni-axial and the bi-axial strength points are marked.

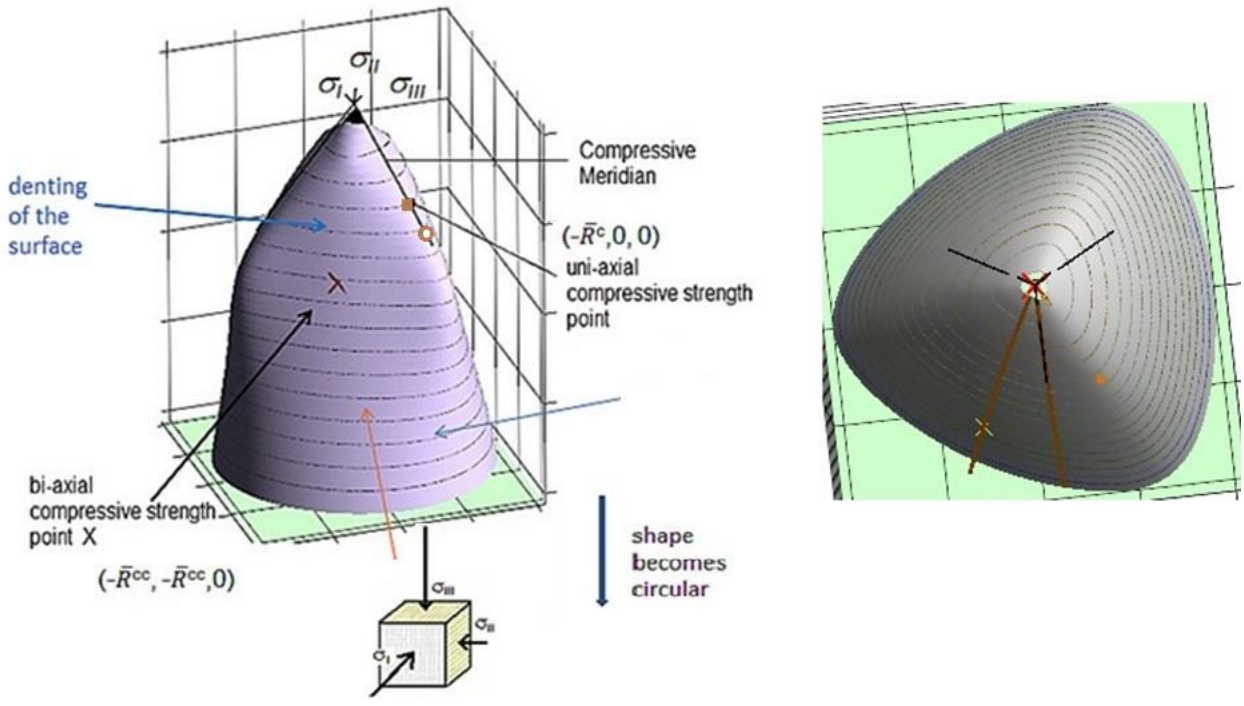

Fig.8: UHPC, Side and top view of the fracture failure body with indicated cross-sections I_1 = constant; fracture stress states ■, ■ . *The three principle axes can be exchanged. m = 2.6.*

3D-compressed isotropic brittle, dense materials have some benefit. This shall be substantiated.
In the IFM-test data set two informative stress states could be found

$$(\sigma_I\,,\ \sigma_{II}\,,\sigma_{III}\,)^T = (-160,\ 0,0)^T\ MPa \quad \text{and} \quad (\sigma_I\,,\ \sigma_{II}\,,\sigma_{III}\,)^T = (-224\ -6,\ -6,\ -6)^T\ MPa.$$

These two measured fracture stress states ■, o are depicted on the fracture body, defined by *Eff* = 100%, help to explain the designations 'strength' and 'multi-axial strength-carrying capacity':
Essential for the designer is that a small bi-axial (confined) compression of -6 MPa lets increase the tolerable axial loading from 160 MPa to 230 MPa. For both the cases *Eff* remains constant at 100% which is the maximum material stressing effort and which defines the surface of the fracture body. There is no increase of the value of the standard compressive strength R^c , because R^c is specified as uni-axial fracture stress linked to specified test conditions.
In this context shall be mentioned, the term overexertion ('Über-Anstrengung') of a material is a fictitious designation. After onset of fracture the material either falls apart or can still carry some loading in the case that for the then strain-controlled critical material locus strain softening is permitted by a surrounding less stressed vicinity. *Eff* still remains 100% because the maximum carrying stress is identical to the reduced (degraded) fracture stress of the associated distinct point on the strain softening curve, the fracture body is shrunken. The lower stress fits with the degraded strength capacity.

LL: The material stressing effort Eff cannot exceed 100%.

Fig.9 displays measured 2D test data of Normal Concrete, provided by Dr. Silke Scheerer, IfM, TU-Dresden. It depicts the wide scatter of the multi-axial compression tests, which influences the statistically reduced design strength significantly.

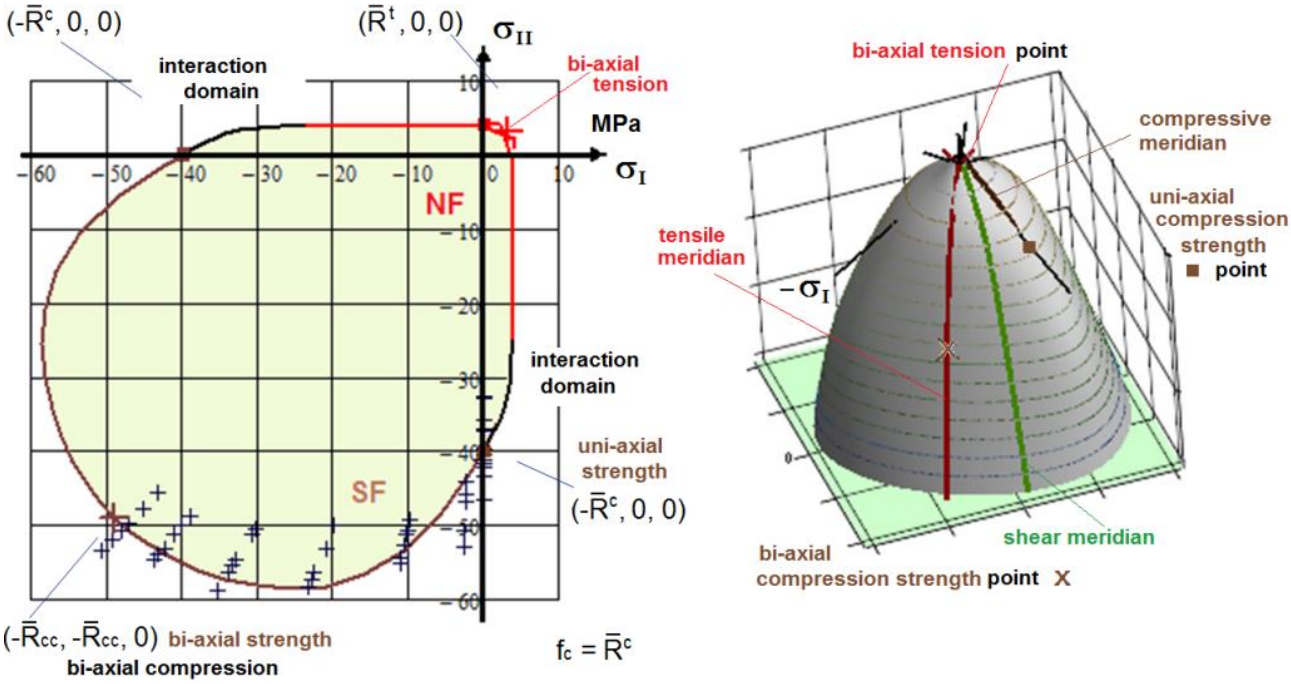

Fig.9: Normal Concrete, 2D-test data set in the principle stress plane with plain separated mode failure curves and after interaction of the two mode failure curves; (right) Fracture body with the basic three meridians and some strength points

4.2 ***Onset of Crushing Fracture of an isotropic, porous material***

In *Table 2* all the FMC-based SFCs are listed, to be applied in tensile and in compression domain, for mapping the course of foam material test data.

Mapping has to be performed in the principal stress plane by applying the 2D-reduced 3D-SFCs, because the test data set was 2D only. Hence one must keep in mind the 3D-failure body depends on 2D-derived model parameters. Rohacell 71 IG foam *[data, courtesy DKI and LBF-Darmstadt, V. Kolupaev]*

Table 2: SFC Formulas for NF and CrF

Tension	Compression
$F^{NF} = \dfrac{\sqrt{4J_2 - I_1^2/3} + I_1}{2\cdot \bar{R}^t} = 1$	$F^{CrF} = \dfrac{\sqrt{4J_2 - I_1^2/3} - I_1}{2\cdot \bar{R}^c} = 1$
$Eff^{NF} = c^{NF}\cdot \dfrac{\sqrt{4J_2\cdot\Theta^{NF} - I_1^2/3} + I_1}{2\cdot \bar{R}^t} = \sigma_{eq}^{NF}/\bar{R}^t$ and	$Eff^{CrF} = c^{CrF}\cdot \dfrac{\sqrt{4J_2\cdot(\Theta^{CrF}) - I_1^2/3} - I_1}{2\cdot \bar{R}^c} = \sigma_{eq}^{CrF}/\bar{R}^c$

Two-fold failure danger can be modelled by using the well known invariant J_3 including d = non-circularity parameter

$\Theta^{NF} = \sqrt[3]{1 + d^{NF}\cdot\sin(3\vartheta)} = \sqrt[3]{1 + d^{NF}\cdot 1.5\cdot\sqrt{3}\cdot J_3\cdot J_2^{-1.5}}$ and $\Theta^{CrF} = \sqrt[3]{1 + d^{CrF}\cdot\sin(3\vartheta)} = \sqrt[3]{1 + d^{CrF}\cdot 1.5\cdot\sqrt{3}\cdot J_3\cdot J_2^{-1.5}}$

Equation of the fracture body: $Eff = [(Eff^{NF})^m + (Eff^{CrF})^m]^{m^{-1}} = 1 = 100\%$ total effort, interaction

c^{NF}, Θ^{NF} from the two points ($\bar{R}^t$, 0, 0) and ($\bar{R}^{tt}$, $\bar{R}^{tt}$, 0) or by a minimum error fit, if data available, c^{CrF}, Θ^{CrF} from the two points (-$\bar{R}^c$, 0,0) and (-$\bar{R}^{cc}$, -$\bar{R}^{cc}$, 0) or by a minimum error fit

The failure surface is closed at the ends by assumed caps.

LL: The SFC for Rohacell 71 IG foam can be also used for the similar behaving concrete stone!

Fig.10 depicts the mapping of the 2D test data set. One clearly sees how the interaction equation maps the plain failure curves and the transition domain between.

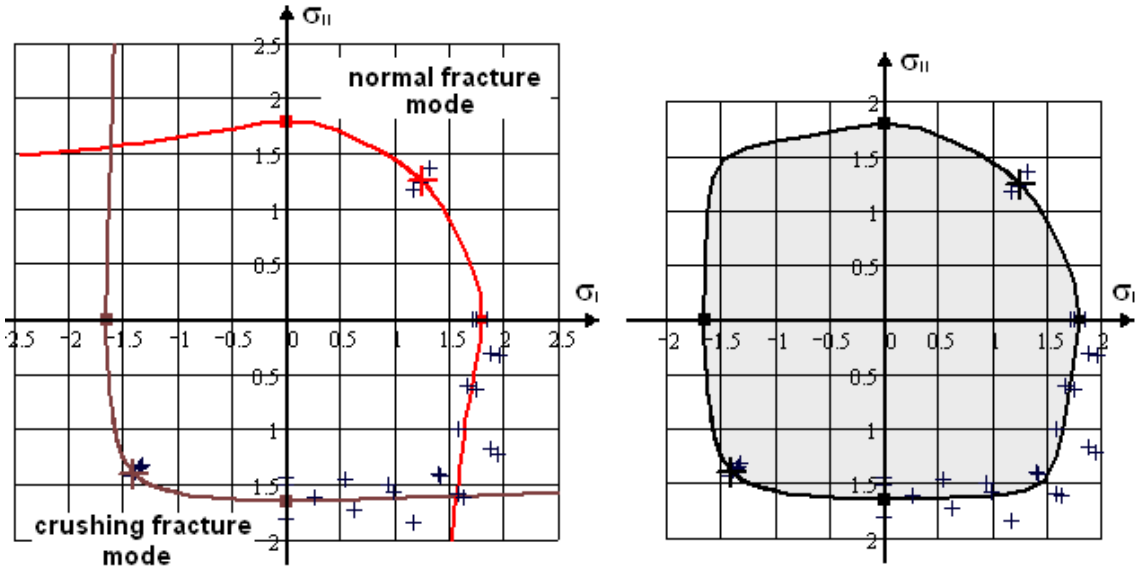

Fig.10: Rohacell 71 IG foam, 2D-test data set of the principle stress plane (oblique cross-section of the body) with plain separated mode failure curves and - right - after interaction of the two mode failure curves

Fig.11 below shows two views of the obtained fracture (failure) body. Due to missing 3D fracture test data the caps had to be assumed. The three meridians and the directions of the three principal axes are indicated. The extreme non-rotational fracture body shows a big skewness.

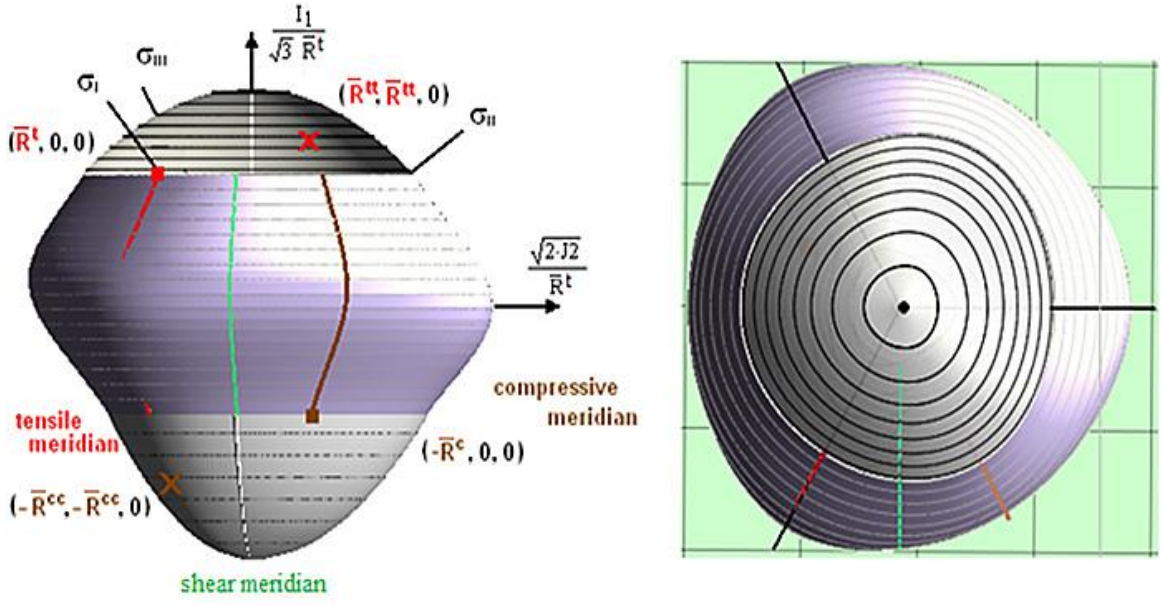

Fig.11: Rohacell 71 IG foam, side view and top view of the fracture failure body

Fig.12 clearly outlines the oppositely turned dent positions for $I_1 > 0$ and $I_1 < 0$.

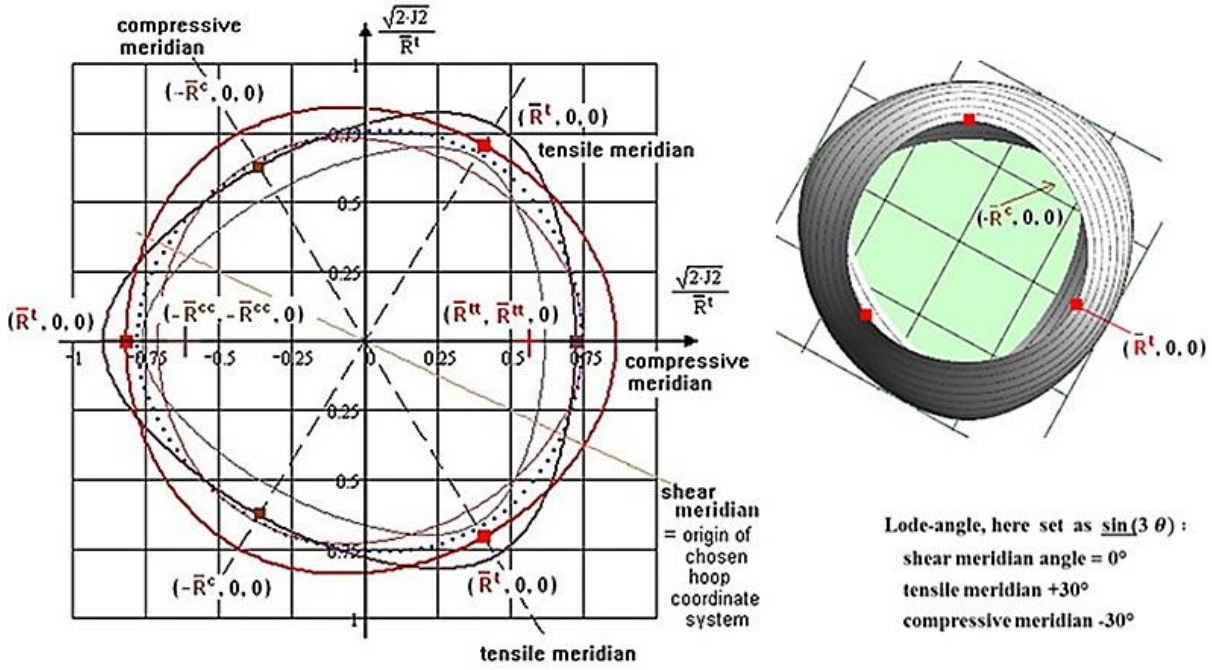

Fig.12: Rohacell 71 IG foam, I_1=constant (hoop) cross-sections of the fracture body. View downward from cross-section cut at tensile strength level

5. FMC-Application to Normal Yielding, Tension (crazing of PMMA)

5.1 General

Glassy (amorphous, brittle) polymers like polystyrene (PS), polycarbonate (PC) and PolyMethylMethacrylate (PMMA, plexiglass) are often used structural materials. They experience two different yield failure types, namely crazing and shear stress yielding that is often termed shear-banding, too. Crazing may be linked to Normal Yielding (NY) which precedes crazing-

following fracture. Crazing occurs with an increase in volume and shear banding does not. Therefore, the dilatational I_1^2 must be employed in the approach for tension $I_1 > 0$. Under compression, brittle amorphous polymers usually shear-band (SY) and with it they experience friction. Therefore, I_1 must be employed in the approach for $I_1 < 0$ in order to consider material internal friction. For obtaining the complete yield failure body its parts NY and SY are to interact, as still performed for concrete before.

Reminder on HMH-linked 'Mises-cylinder' for 'Onset-of-Shear Stress Yielding SY*: There is no friction acting and therefore yield strengths for compression and tension are the same* $R_{0.2}^{c} = R_{0.2}^{t}$ *(≡* $R_{p0.2}$*, in which the superfluous suffix* $_p$ *practically has nothing to do with proportional). HMH means frictionless yielding and therefore it forms a cylinder.*

Crazing involves the formation of fibrils bridging two neighboring layers of the un-deformed polymer. These subsequently elongate and locally fail which leads to a formation or an elongation of an existing micro-crack, *Fig.13*. This micro-crack can be simulated under Fracture Mode-I loading conditions, setting now $K_{Ic} \equiv K_{Icr}^{(t)}$ as indicated.

The failure type crazing shows a curiosity under tensile stress states: A non-convex shape exists for Onset-of-Crazing ($\bar{R}_{NY}^{t}$). NY is followed by the crazing-driven fracture NF_{NY} for which - due to the similar shape – the NY-SFC can be used too. Under compressive stress states the usual shear band yielding SY occurs and later as final shear fracture SF occurs. For both, SY and SF, the same SFC can be applied.

Note: Due to the fact that the Onset-of Crazing and the Onset of shear yielding associated stresses ("strengths") are not accurately described the denotations $\bar{R}_{NY}^{t}$ *and* $\bar{R}_{0.2}^{c}$ *are used. This has no influence on the logic followed here.*

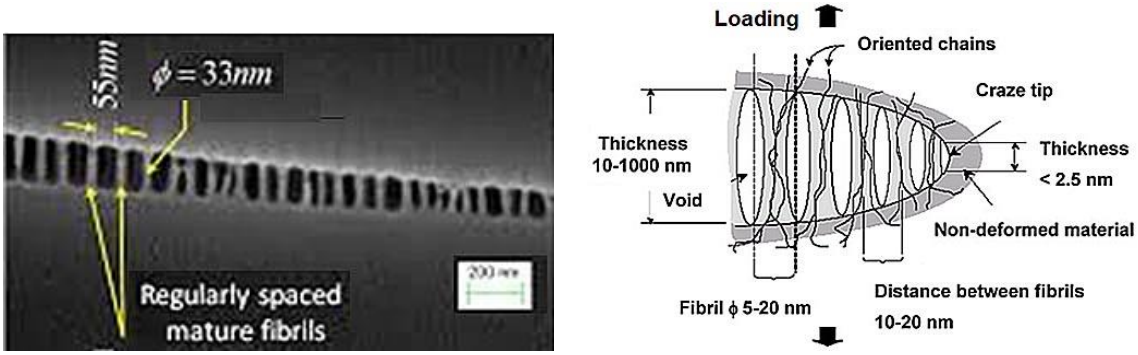

Fig.13: PMMA, SEM image of a craze in Polystyrene Image, created by Y. Arunkumar

5.2 Available test data sets for PMMA

For the validation of the FMC-based SFC for PMMA two data sets were available, one NY-2D-data set from Sternstein-Myers [Ste73] and a SY-3D-data set from Matsushige [Mat73].
These two sets, depicted in *Fig.14*, are unfortunately of different origin: (1) Sternstein-Myers performed bi-axial experiments on craze initiation on the surface of thin-walled cylinders (tubes). The loadings were axial tension + internal pressure and tension + torsion. Test temperature was 60° C. Therefore, following literature, to match with Matsushige's ambient temperature 23°C data, from consistency reasons the value of $\bar{R}_{NY}^{t}$ is to increase to become comparable with Matsushige. (2) Matsushige performed tri-axial experiments on sealed (surface crazing is hindered) solid rods at 23° C, under axial tension + p_{hyd}. The test specimen was pressurized within a chamber. This series along the tensile meridian, characterized by $\sigma_I > \sigma_{II} = \sigma_{III}$, contains the bi-axial point

($-\bar{R}^{cc}_{0.2}$, $-\bar{R}^{cc}_{0.2}$, 0). In comparison to the thin tube the solid rod experiences more bulk crazing than the more dangerous surface crazing. This is essential for test data evaluation.

Of special interest for the demonstration of a qualified mapping by the SY-SFC and the NY-SFC is the mapping of tensile meridian and compressive meridian as the essential cross-sections of the yield failure body. The definitions of the meridians are given below, associated test stress states are formulated in principal stresses and in mathematical stresses:

tensile meridian compressive meridian

$$(\sigma^{t}_{ax} - p_{hyd}, -p_{hyd}, -p_{hyd}) = (\sigma_I, \sigma_{II}, \sigma_{III}) \rightarrow \sigma_I > \sigma_{II} = \sigma_{III} \;\Leftrightarrow\; (-p_{hyd}, -p_{hyd}, \sigma^{c}_{ax} - p_{hyd}) = (\sigma_I, \sigma_{II}, \sigma_{III}) \rightarrow \sigma_I = \sigma_{II} > \sigma_{III}$$

A 2D-data set and a 3D-data set can be put together in a Lode-Haigh-Westergaard diagram. The two data sets clearly outline crazing NY (Sternstein) and shear banding SY (Matsushige) and therefore can serve for mapping.

A harmonization of the two data sets is necessary: After transferring into MPa, the Matsushige fracture stress values were much higher than the Sternstein ones. Following Sternstein et al the threshold stress value required for crazing (ten minutes hold-time) is about 3900 psi (1000 psi = 6.89 MPa) and for ambient temperature about 5500 psi is guessed, extrapolating his curve approximately. This has the consequence to increase the Sternstein test data by a correction factor of $f \approx 5500/3900$. The choice finally was $f = 1.3$.

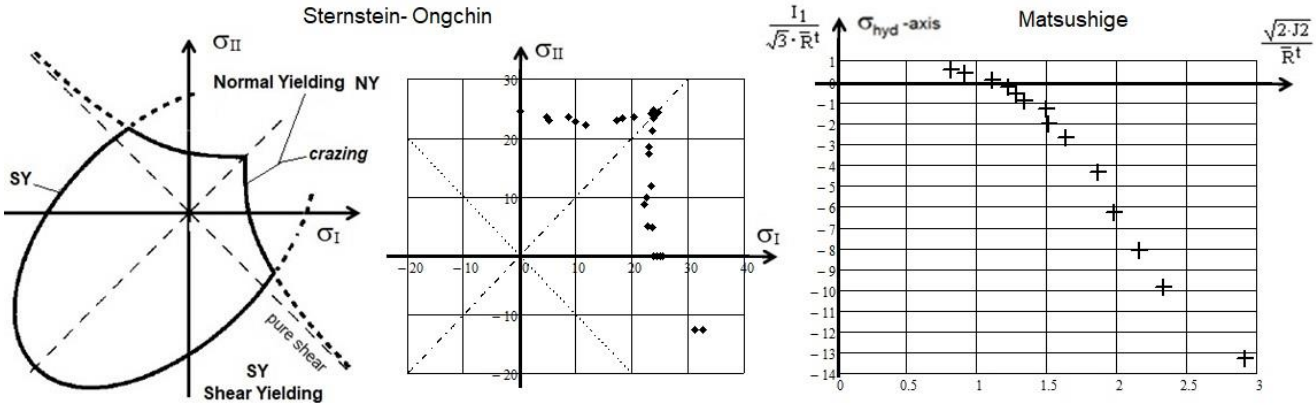

Fig.14: (left) Sternstein's mapping idea with his 2D test data set in the principal stress plane, (right) Matsushige 3D-PMMA test data set rendered in Haigh-Westergaard-Lode coordinates. Test data sets from Sternstein-Myers and Matsushige were harmonized by the author on basis of literature

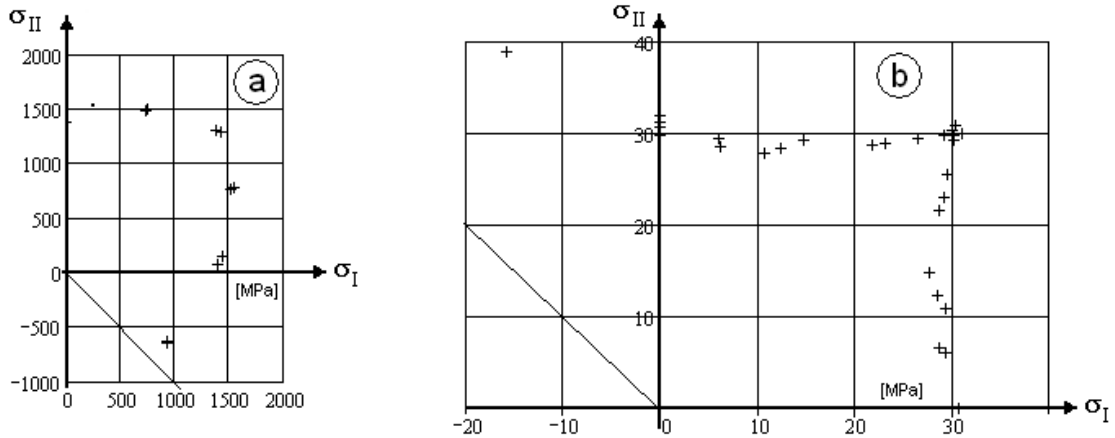

Fig.15: PMMA, Tension domain with (a) Onset-of-Shear Yielding test data for a steel, SY, for comparison; (b) Onset-of-Crazing NY. Strength points: ($\bar{R}^{t}_{NY}$, 0, 0), ($\bar{R}^{tt}_{NY}$, -$\bar{R}^{tt}_{NY}$, 0), ($\bar{R}^{c}_{0.2}$, 0, 0)

Fig.14 and *Fig.15* clearly outline, that the course of test data needs to be differently mapped for the convex-shaped SY and the concave-shaped NY.
In the interaction zone from crazing to shearing a brittle-to–ductile transition occurs, p_{hyd} induces the transition from NY to SY by suppressing crazing.

5.3 Formulas and visualization Onset of Yielding NY with SY: isotropic, dense material

Traditional SFCs describing yielding are related to Hencky-Mises-Huber (HMH hypothesis (or Mises, in short) and to the 'corner-suffering' Tresca hypothesis. Tresca was preferred in the past due to its less computational effort and is still often mistakenly used as strength fracture failure condition seduced by its failure surface shape in tension in the principal stress plane. HMH delivers an ellipse as the cylinder's cross-section, whereas Tresca leads to a hexagon, see *Fig.16*.

Normal Yielding (*PMMA*) **Shear Yielding**

Hyperboloide Paraboloide

$$F^{NY} = \frac{x^2}{c_2^{NY2}} - \frac{(y - c_1^{NY})^2}{c_3^{NY2}} = 1 \text{ with } x = \frac{\sqrt{2 \cdot J_2 \cdot \Theta^{NY}}}{\bar{R}^t_{NY}},\ y = \frac{I_1}{\sqrt{3} \cdot \bar{R}^t_{NY}} \text{ for } I_1 > 0 \Leftrightarrow F^{SY} = c_1^{SY} \cdot \frac{3J_2 \cdot \Theta^{SY}}{\bar{R}^{c\ 2}_{0.2}} = 1 \text{ for } I_1 < 0$$

Considering bi-axial strength (failure mode occurs twice, $\Theta \neq 1$). In Effs now, if possible.

$$Eff^{NY} = \frac{c_3^{NY} \cdot \sqrt{-c_2^{NY2} \cdot y^2 + \Theta^{NY2} \cdot (c_3^{NY2} + c_1^{NY2}) \cdot x^2} + c_2^{NY} \cdot c_1^{NY} \cdot y}{c_2^{NY} \cdot (c_3^{NY2} + c_1^{NY2})} \leftrightarrow Eff^{SY} = \sqrt{c_1^{SY} \cdot \frac{3J_2 \cdot \Theta^{SY}}{\bar{R}^{c\ 2}_{0.2}}} = \sigma^{SY}_{eq} / \bar{R}^c_{0.2},\ Eff^{Mises} = \sqrt{\cdot \frac{3J_2 \cdot 1}{\bar{R}^{c\ 2}_{0.2}}}$$

Onset of Crazing = Normal Yielding NY (for fracture similar)

c^{NY}, Θ^{NY} from the two points $(\bar{R}^t_{NY}, 0, 0)$ and $(\bar{R}^{tt}_{NY}, \bar{R}^{tt}_{NY}, 0)$ Θ^{SY} from the point $(-\bar{R}^{cc}_{0.2}, -\bar{R}^{cc}_{0.2}, 0)$

Two-fold failure danger can be modelled by using the well known invariant J_3 including d = non-circularity parameter

$$\Theta^{NY} = \sqrt[3]{1 + d^{NY} \cdot \sin(3\vartheta)} = \sqrt[3]{1 + d^{NY} \cdot 1.5 \cdot \sqrt{3} \cdot J_3 \cdot J_2^{-1.5}} \text{ and } \Theta^{SY} = \sqrt[3]{1 + d^{SY} \cdot \sin(3\vartheta)} = \sqrt[3]{1 + d^{SY} \cdot 1.5 \cdot \sqrt{3} \cdot J_3 \cdot J_2^{-1.5}}$$

Lode angle ϑ, here se tas $\sin(3 \cdot \vartheta)$ with 'neutral'shear meridian angle 0°; tensile meridian angle 30°; com. m. angle -30°

A yield body is rotational symmetric if $\Theta = 1$

Equation of the yield failure body: $Eff = [(Eff^{NY})^m + (Eff^{SY})^m]^{m^{-1}} = 1 = 100\%$ total effort, interaction

$0 < d^{NY} < 0.5$, $0 < d^{SY} < 0.5$, meridian angles $\vartheta°$: $\bar{R}^t_{0.2}$, 30° ; $\bar{R}^{tt}_{0.2}$, -30°; $\bar{R}^c_{0.2}$, -30°; $\bar{R}^{cc}_{0.2}$, 30°

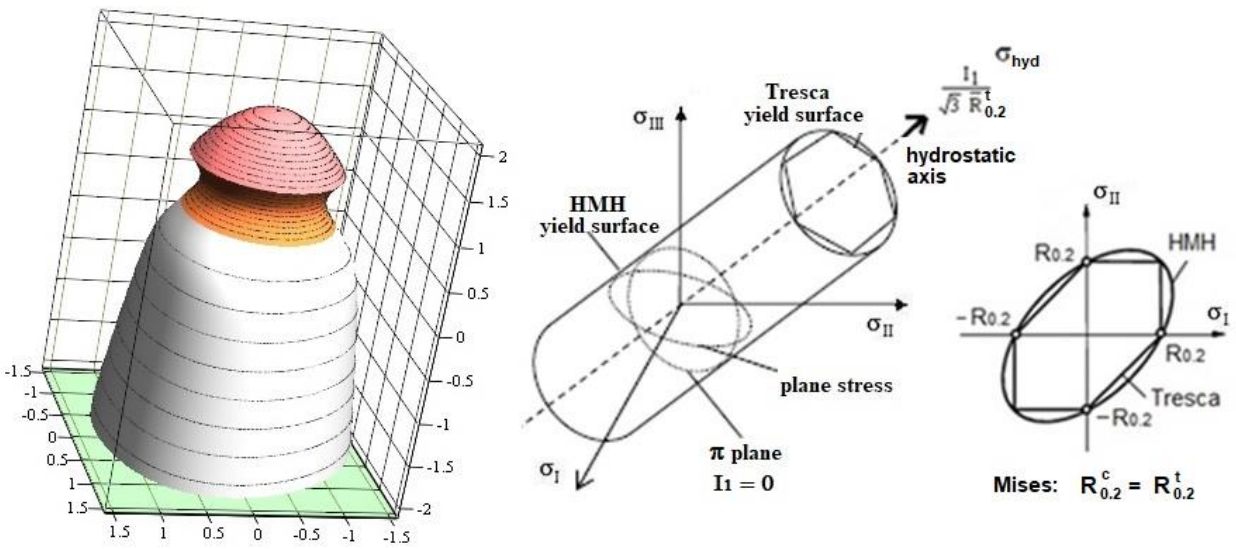

Fig.16: PMMA, (above) Formulas for NY and SY; (left) Onset-of-Yield surface (NY with SY) and for comparison Hencky-Mises-Huber with the Tresca yield surface (engineering yield strengths are used)

The NY yield failure body is as it is an isotropic material also 120°-symmetric in the deviator plane. This is captured by $\Theta(J_3)$, again. I_1^2 (y^2) stands for the experienced volume change. Above formula for the failure body is new.

In the following two figures, *Fig.17*, the two main meridians as axial-parallel cross-sections of the failure body are presented (upper part) and the I_1 = constant yield failure curves (lower part).

- In the upper part the plain failure curves are shown and the magenta cloured curves in the transition domain after interaction. $\bar{R}_{SY}^{c}$ is not clearly defined by Sternstein and Matsushige, but this is not essential, because NY-mapping is the objective. So, instead of the not defined $\bar{R}_{NY}^{t}$, $\bar{R}_{SY}^{c}$ the usual denominations for strengths are kept.
- In the lower part the 'I_1 = constant yield failure curves' are displayed for the tensile and the uni-axial compressive strength and the bi-axial strength capacity. In addition the most inner ring of the hyperboloid is included (orange).

Tensile Meridian Compressive Meridian

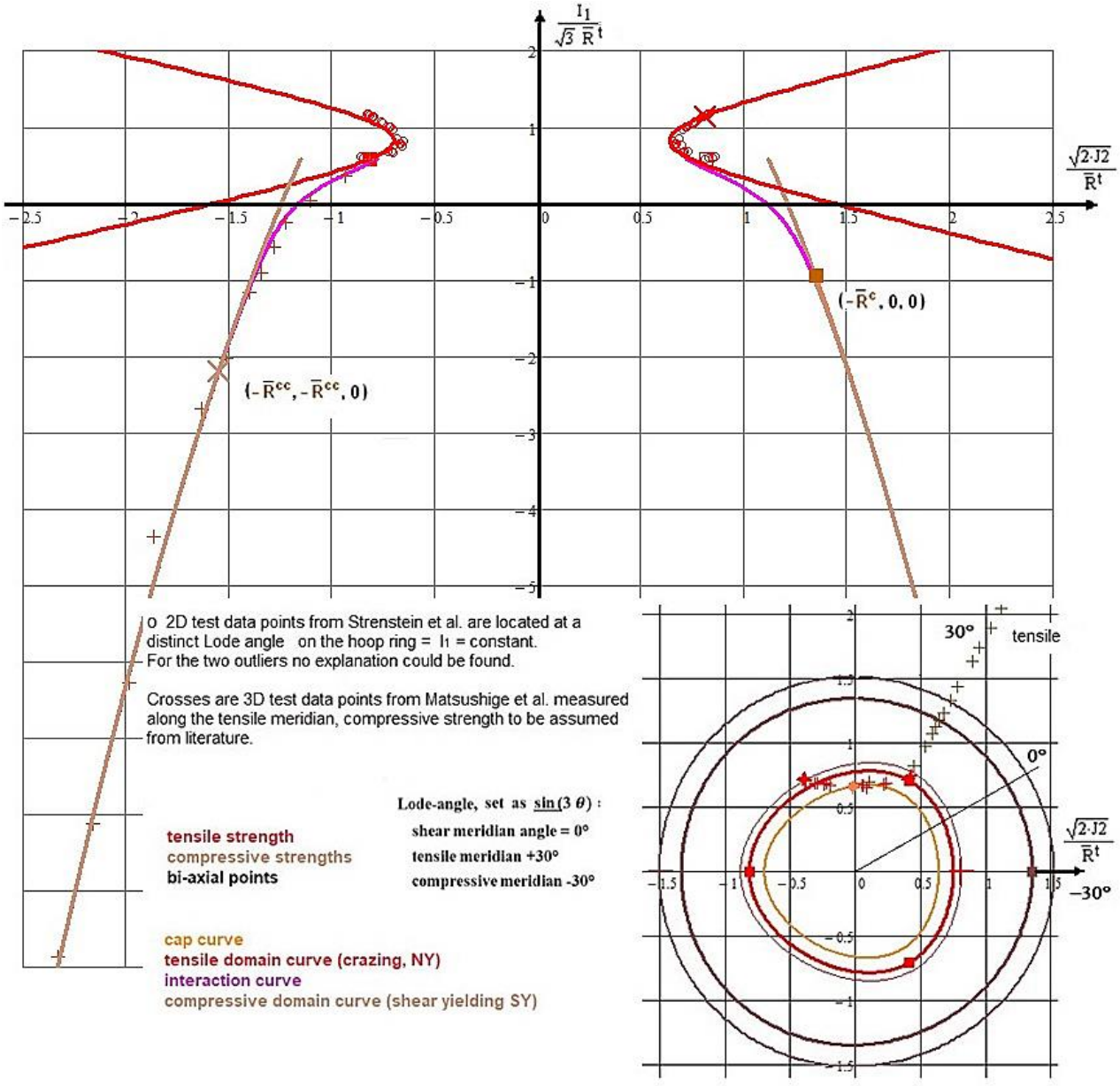

Fig.17: Tensile and compressive meridians of the fracture body (not optimized, the most negative test points are not shown in the figure); (below) I_1 = constant cross-sections of the NY-SY-body. *m =5.2*

*The figure before shows that the Matsushige tests were run along the compressive meridian.
*Due to the 120°-symmetry the inserted test points are three times on the hoop plane present.

For the derivation of the tensile *fracture* failure body – due to the similar shape – the NY-SFC can be employed too, viewing yield curve and fracture curve presented in [Bre79]. For the compression part is similarly valid, SY → SF.

Note: Many years ago the author constructed a hyperboloid function that could map straight test data courses in the principal stress plane (NF-SFC, see the examples before) and convex dents. The NY-SFC now enables to manage concave outward dents, Fig.18.

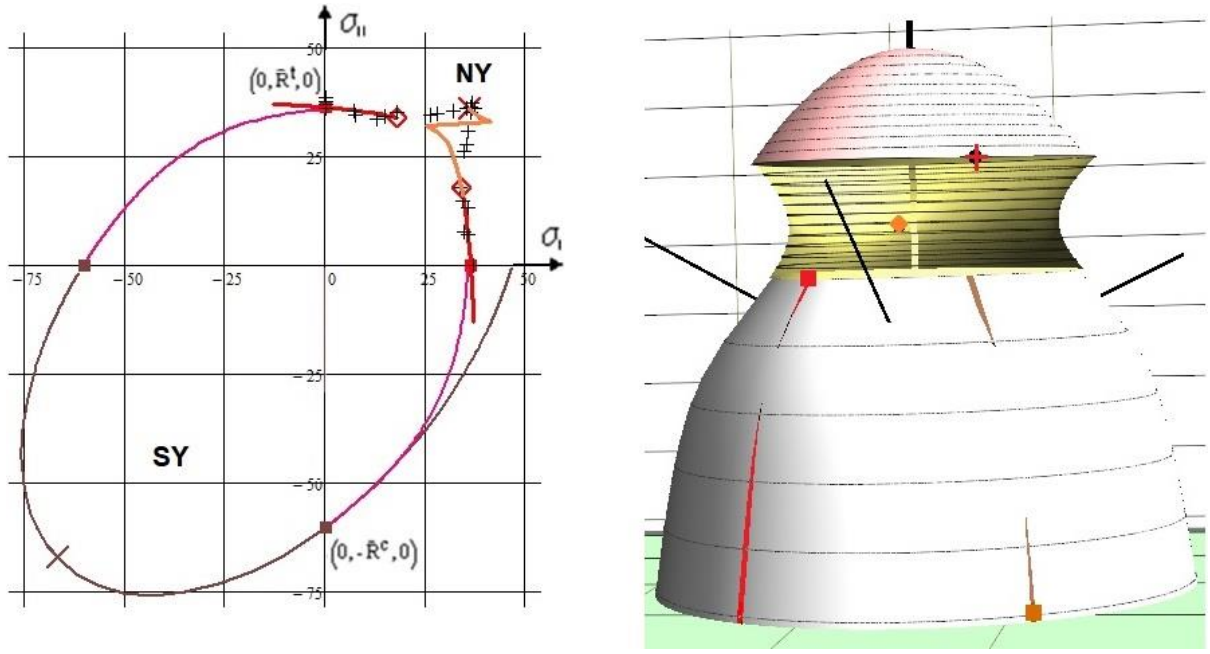

Fig.18: PMMA, (left) Harmonized test data in tension and compression domain with and without interaction; (right) depiction of the fracture body shape with some representative points

For a first time mapping of the PMMA-NY was successful.

The visualization with the used Mathcad 15 code (35 DIN A4-pages application) is challenging considering the solver that faces a concave 2D principal stress plane situation instead of a usual convex one

However, the success was clouded. Also after a huge effort, the author unfortunately could not obtain a mapping of the upper test data in the first quadrant with the used Mathcad 15 code. The computed mapping curve remains a zig-zag even after several different computational approaches as for example from the outer bi-axial point X to the more inner points! Why does the solver in the lower tensile part of the yellow colored failure surface work and in the upper not (zig-zag curve)? The points on the surface of the right figure cannot explain this. Can the Mathcad solver capture such concave situations?

6. Existence of a Stress Intensity Factor under Compression, K_{IIcr}^{c} ?

6.1 General

Fracture Mechanics FM is the field of mechanics concerned with the study of the propagation of cracks. These cracks might have been there from the beginning or are formed under loading. Final fracture occurs when cracks propagate up to a limit state. The critical stress intensity factor SIF K_{Ic}

(later necessarily to be termed K_{Icr}^{t}) is found in a plane strain condition, and is accepted as the defining (basic) property in Linear Elastic Fracture Mechanics, considering tension.

Comparing strength mechanics and fracture mechanics a question of the author is: "*Are there any links between them?"*

- Normal fracture NF acts perpendicular to the mathematically highest stress ('most positive') σ_I. If a centrally cracked test specimen is loaded at a certain level, the crack grows in the fracture plane. R^t and K_{Icr}^{t} correspond, *Fig.19*.
- Shear Fracture SF occurs under a compressive stress, that causes a critical combination of the Mohr stresses σ_n,τ_n , leading to a fracture plane angle Θ_{fp}^{c}.

Note: In order to cope with the generally in structural engineering used indexing, one has to keep ^{c} *for compression and* ^{t} *for tension and set critical* $_{cr}$ *for all fracture-mechanical quantities instead of the suffix* $_{c}$*, see further the Annex.*

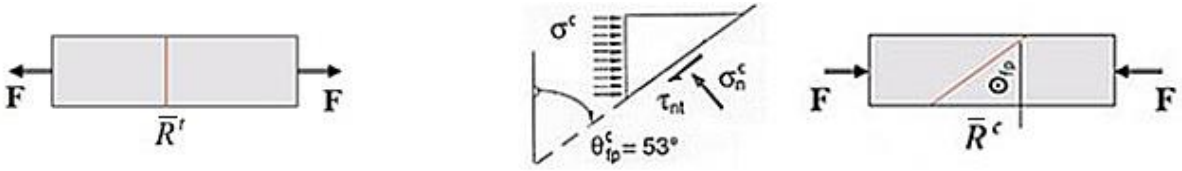

Fig.19: Fracture angles of brittle material under tension and compression; (left) NF with tensile strength, (right) SF with compressive strength

Connected question:

*"Is there a crack plane-linked '*transition'* from 'Without crack' (strength mechanics) to 'With crack' (fracture mechanics) also in the compression domain* $I_1 < 0$ *?*

A first response is: "From material symmetry information one could conclude that the number of fracture toughnesses or crack resistances, which are equivalent to the (basic) critical SIFs, is the same as the number of strength fracture resistances, namely R^t and R^c. The number of the (basic) critical SIFs may be also two, namely $K_{Icr}^{t} \equiv K_{Ic}$ and K_{IIcr}^{c}".

Focusing tension: According to the multi-dimensional stress state present cracks in materials usually do not propagate along their original crack plane but under so-called 'mixed mode loading' on curved paths in which the specific singularity situation at the crack tip is decisive.
The decomposition of a loading state into the three basic deformation modes, the fracture mechanics Modes-I, -II, -III, was introduced by Irwin and the different deformations he indicated by arrows, see *Table 3*. These deformation states are usually linked in literature, however, to crack driving loadings and further to stresses: Mode I – Opening mode (a tensile stress normal to the plane of the crack), Mode II – Sliding mode (a shear stress acting parallel to the plane of the crack and perpendicular to the crack front), and Mode III – Tearing mode (out-of-plane shear loading).

Structural engineers, who apply FM tools for predicting lifetime by damage tolerance means, are used to think in stresses. Therefore they claim "*The fracture mechanics modes II and III are not in local equilibrium*". Bouquet's faces clearly depict this in *Table 3*. Of course, the consequence of being not in equilibrium is a turning of the original crack-plane into a direction normal to the principal *tensile* stress σ_I.

LL: Mode I delivers a real ('basic') fracture resistance property generated under a tensile stress. Both the Modes II K_{IIc}*, and III* K_{IIIc} *do not show a stable crack plane situation but are nevertheless essential FM model parameters to capture 'mixed mode loading' for performing a multi-axial assessment of the far-field stress state.*

Focusing compression: There is another domain, namely geo-engineering and rock fracture mechanics, that is pretty decoupled from the tension domain in mechanical engineering, where FM plays a big role. The cracks to be faced here under compression loads are many meters long and more. Here, K_{IIcr}^{c} is the focus but usually prevented by the secondary wing-cracking accompanied by splitting! Therefore, the situation to detect it and to measure it is complicated.
At the crack tip a local perturbation caused by for instance a stiff or a too large grain can change the local stress singularity situation by not generating a desired 'fine grained, homogeneous micro-structure'. Then the modelling-desired ideal homogenization state is violated and splitting of brittle test specimen will occur.

Note: Generally speaking, it is with the Mode-II fracture toughness K_{IIcr}^{c} like with strength. One says compressive failure, but actually shear (stress) failure is meant, compressive stress is only the descriptive term.

Author's postulate employing crack path stability:
Only a stable, crack growth plane-associated SIF is a 'basic' FM property.

6.2 Information from literature on the existence of K_{IIcr}^{c}

Literature seems to support the author who assumes that there are two basic critical SIFs, only. His more detailed definition of such a basic SIF is: ***The direction of the crack progress remains in the distinct plane if the stress situation remains the same and the singularity situation at the crack tip is not changed by for instance a large grain*** *(then it is not a theoretically ideal situation anymore).* In other words, the crack increases in its original plane, if the stress state remains in the crack case as in the (non-cracked) strength case. This should be valid in the compression domain, too.

- Tension domain: One knows from K_{Icr}^{t} (tension), that – viewing the angle - it corresponds to R^{t}.
- Compression domain: The not generally known second basic SIF K_{IIcr}^{c} seems to exist under ideal conditions. It corresponds to shear fracture SF happening under compressive stress and leading to the angle Θ_{fp}^{c}. The crack surfaces are closed for K_{IIcr}^{c}, friction sliding occurs.

The author's postulate "K_{IIcr}^{c} exists" is firstly supported by an experiment with cracked test specimens under compression and secondly by a still available K_{IIcr}^{c} formulation substantiated by the maximum value of the material stressing effort *Eff* for $\alpha = 90 - \Theta_{fp}^{c}$.

I Some experimental proofing of K_{IIcr}^{c}

A first proof of the author's postulate could be: There is a minimum value of the compressive loading at a certain fracture angle. This means that the K_{IIcr}^{c} becomes a minimum, too. Liu et al performed in [Liu14] tests using a cement mortar material. They describe the test investigations as "The specimens were square plates of 180mm×180mm×50mm, with three collinear artificial and penetrated cracks, which measure 20 mm in length. The ratio of cement, sand, and water is 1 : 1 : 0.35 by weight. The cracks were made by using a 0.1 mm film, placed during casting. Curing period was 28 days. Under controlled temperature 130°C for 2hrs, the films can be easily pulled out. The crack length and their interval distance are the same and equal 1.0 cm. The test specimens were loaded by a tri-axial loading device: The vertical loading is the major principal stress σ_1 and the two horizontal confining stresses are kept as constants during the process of vertical loading.

Table 3: Fracture mechanics modes, stress states and (down) possible crack angles (α = inclination angle, angle $\Theta_{fp}{}^{c}$ is measured in compression test, differently defined)

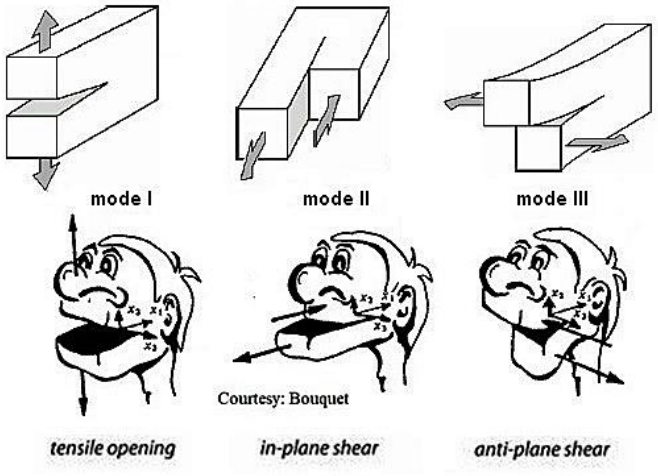

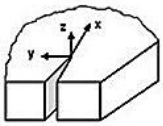

structural stresses $\{\sigma\} = (\sigma_x, \sigma_x, \sigma_x, \tau_{yz}, \tau_{xz}, \tau_{xz})^T$

principal stresses $\{\sigma\}_{prin} = (\sigma_I, \sigma_{II}, \sigma_{III})^T$

Mohr stresses $\{\sigma\}_{Mohr} = (\sigma_\ell, \sigma_n, \sigma_n, \tau_{nt}, \tau_{t\ell}, \tau_{n\ell})^T$

Tension:

Full 3D-stress state $\{\sigma\} = (\sigma_x, \sigma_y, \sigma_z, \tau_{yz}, \tau_{zx}, \tau_{xy})^T \equiv (\sigma_I, \sigma_{II}, \sigma_{III})^T$

with mathematical stresses $\sigma_I >$ (more positive) $\sigma_{II} > \sigma_{III}$

$\{\sigma\} = (0, \sigma_y, 0, 0, 0, 0)^T \equiv (\sigma_I, 0, 0)^T \Rightarrow K_{Ic} = K^t_{Icr}$ (stable crack angle $\Theta_{fp} = 0°$ $\leftrightarrow$ strength: $(\sigma^t_n, 0)^T$ with $\Theta_{fp} = 0°$ (fracture angle, NF)

$\{\sigma\} = (0, 0, 0, 0, 0, \tau_{xy})^T \equiv (\sigma_I, 0, \sigma_{III})^T \Rightarrow K_{IIcr} \leftarrow$ (no stable crack angle)

$\{\sigma\} = (0, 0, 0, \tau_{yz}, 0, 0)^T \equiv (\sigma_I, 0, \sigma_{III})^T \Rightarrow K_{IIIcr} \leftarrow$ (no stable crack angle)

if fully ductile, dense: $\rightarrow \Theta_{fp} = 45°$ inclined yield plane

Full farfield stress states: Superposition possible, if linear problem is applicable,

Mixed Fracture Mode condition: altering angle Θ_{fp} turns into the transversal plane of principal tensile stress

$\{\sigma\} = (0, \sigma_y, 0\ \tau_{yz}, 0, \tau_{xy})^T \equiv (\sigma_I, \sigma_{II}, \sigma_{III})^T \leftrightarrow 3D: (\sigma^t_n, \tau_{nt}, \tau_{n\ell})^T, \Theta_{fp}$(x,y,z)

The fracture mechanics modes II and III cause a turning of the original crackplane.

Compression:

$\{\sigma\} = (\sigma_x, \sigma_y, \sigma_z, \tau_{yz}, \tau_{zx}, \tau_{xy})^T \equiv (\sigma_I, \sigma_{II}, \sigma_{III})^T$

with mathematical stresses $\sigma_I > \sigma_{II} > \sigma_{III}$

$\{\sigma\} = (\sigma_x, 0, 0, 0, 0, 0)^T \equiv (0, 0, \sigma_{III})^T \Rightarrow K^c_{IIcr}$ (stable crack angle is assumed)

$\Theta_{fp}{}^{c}$ ideal crack tip situation presumed $\leftrightarrow$ strength: $(\sigma^t_{ncr}, \tau_{ntcr})^T$ with $\Theta_{fp}{}^{c}$ (SF fracture angle)

$\alpha \neq \Theta_{fp}{}^{c} \leftrightarrow$ strength: $(\sigma^t_n, \tau_{nt})^T$ (no stable crack angle, wing cracks created)

Full farfield stress states: Superposition possible, if linear problem is given.

Different stress states lead to different Mohr stress states and different failure planes Θ_{fp}

$\{\sigma\} = (\sigma_x, 0, 0\ \tau_{yz}, 0, \tau_{xy})^T \equiv (\sigma_I, \sigma_{II}, \sigma_{III})^T \leftrightarrow 3D: (\sigma^c_n, \tau_{nt}, \tau_{n\ell})^T, \Theta_{fp}$(x,y,z)

$\{\sigma\} = (\sigma_x, \sigma_y, 0\ , 0, 0, 0)^T \equiv (\sigma_I, 0, \sigma_{III})^T \leftrightarrow 3D: (\sigma^c_n, 0, \tau_{n\ell})^T, \Theta_{fp}$(x,y,z)

$\{\sigma\} = (\sigma_x, \sigma_y, \sigma_z, \tau_{yz}, \tau_{zx}, \tau_{xy})^T \equiv (\sigma_I, \sigma_{II}, \sigma_{III})^T \leftrightarrow 3D: (\sigma^c_n, \tau_{nt}, \tau_{n\ell})^T, \Theta_{fp}$.

One of the horizontal stresses is denoted σ_3, and the other one σ_2, as shown in Fig.20. In order to avoid the effect of the friction between the specimen and the loading device, the specimen surfaces were smeared with oil before testing".

→ The significant result of this test series is: A minimum value is located at about $\alpha = \Theta_{fp}^{c} \approx 45°$. That fits relatively well. Of course there is some difference between three collinear cracks and a single crack.

The validity of the results, to use them as a proof, would have been improved if the angle $\alpha = 50°$ had been tested, too.

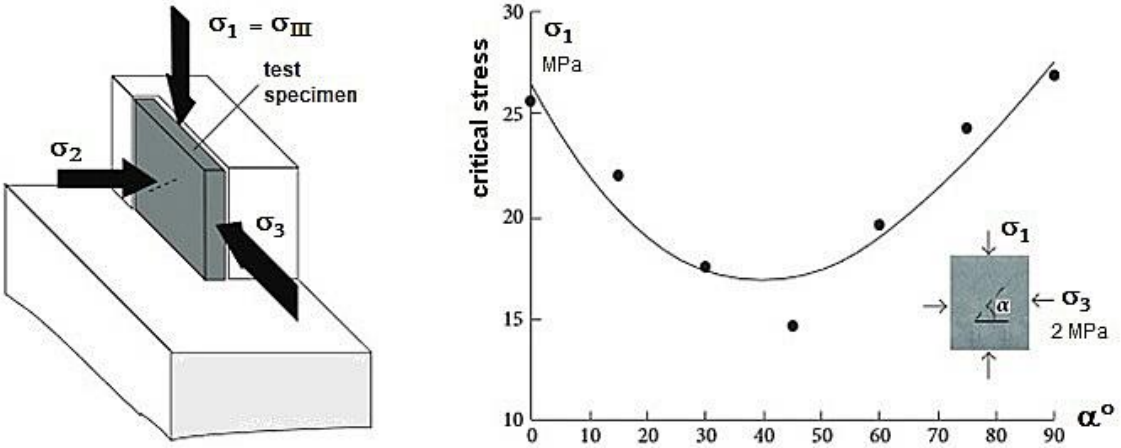

Fig.20: Scheme of the test set-up and of the test points obtained for cement mortar [Liu14], σ_1 represents the mathematical stress σ_{III} (largest compressive stress value). Here literature defines $\Theta_{fp}^{c} = \alpha$

II Formulation (still available) and course of the SIF K_{IIcr}^{c}

The author believes as a second proof for the existence of the fracture toughness K_{IIcr}^{c}, that a formula is still available. PH Melville published in [Mel77] *(literature not got, information from [Pha03])*

$$K_{IIcr}^{c} = \sigma \cdot \sqrt{\pi \cdot a} \cdot \sin(\alpha) \cdot [\cos(\alpha) - \tan(\varphi) \cdot \sin(\alpha)] \quad \text{with}$$

σ = far field stress, a = half crack size, α = flaw (crack) angle and $\tan(\varphi) \cong \mu$.

The SIF depends on the size of the friction value μ. It is the highest, if $\Theta_{fp}^{c} = 90 - \alpha$ *(as defined here)* Fig.21.

The number on the curves in the right figure marks the maximum value of each 'friction' curve.

Exemplarily assuming the usual linear Mohr-Coulomb $tan(\varphi) = \mu = 0.2$ means that $\Theta_{fp}^{c} = 50°$. A check of the special case "ductile" with $\mu = 0$ works as the angle α correctly then becomes the frictionless shear sliding angle or yield angle 45°.

→ For a specific brittle material with its associated friction the SIF K_{II}^{c} becomes highest when $\alpha = 90 - \Theta_{fp}^{c}$. This means this is the friction-dependent critical situation and will lead to further crack growth in this plane.

III When does Onset-of-Failure occur?

From fiber-reinforced laminates is known that as well a strength failure condition SFC as an energy condition must be met at failure onset. For thin layers the strength failure conditions used in Classical Laminate Theory are sufficient, for thicker layers a fracture mechanics condition (SIF) is to apply in order to predict failure of the transverse stresses in the '90°- layers'.

→ The application of a SFC must be checked whether it is 'Necessary' and 'Sufficient'. Principally it is further to check whether any one energy-based condition is on top to take into account, like a LEFM one. Is the energy a minimum one or is K a maximum one?

This means when linking strength and LEFM to investigate the crack growth angle:

* Domain $I_1 > 0$ (tension, classical fracture mechanics):
  The maximum hoop stress in front of the crack-tip rules - after Erdogan-Sih - the growth direction of the crack. This practically means that a SFC for NF is employed when investigating the turning of the crack in front of the crack-tip under multi-axial far field stress states
* Domain $I_1 < 0$ (compression, civil engineering, rock mechanics):
  Could it not be that under compression also a SFC for SF can be employed? This SFC considers the energy at fracture failure. At which fracture angle becomes the SF-SFC a minimum? This can be performed by using the material stressing effort *Eff* in combination with a minimum necessary energy amount $\mathcal{G} = K^2 \cdot (1-\nu^2) / E$. Hence one can pose the questions:
  → At which angle does *Eff* have a maximum? Applying linear Mohr-Coulomb the material stressing effort follows $Eff = \tau_n / (R^\tau - \mu \cdot \sigma_n)$
  → At which angle takes the stress intensity K_{II} a maximum?

This is elaborated in the various pictures in *Fig.21*, right side, with the response:
If the inclination angle corresponds to the fracture angle Θ_{fp}^c , then a critical state is generated.

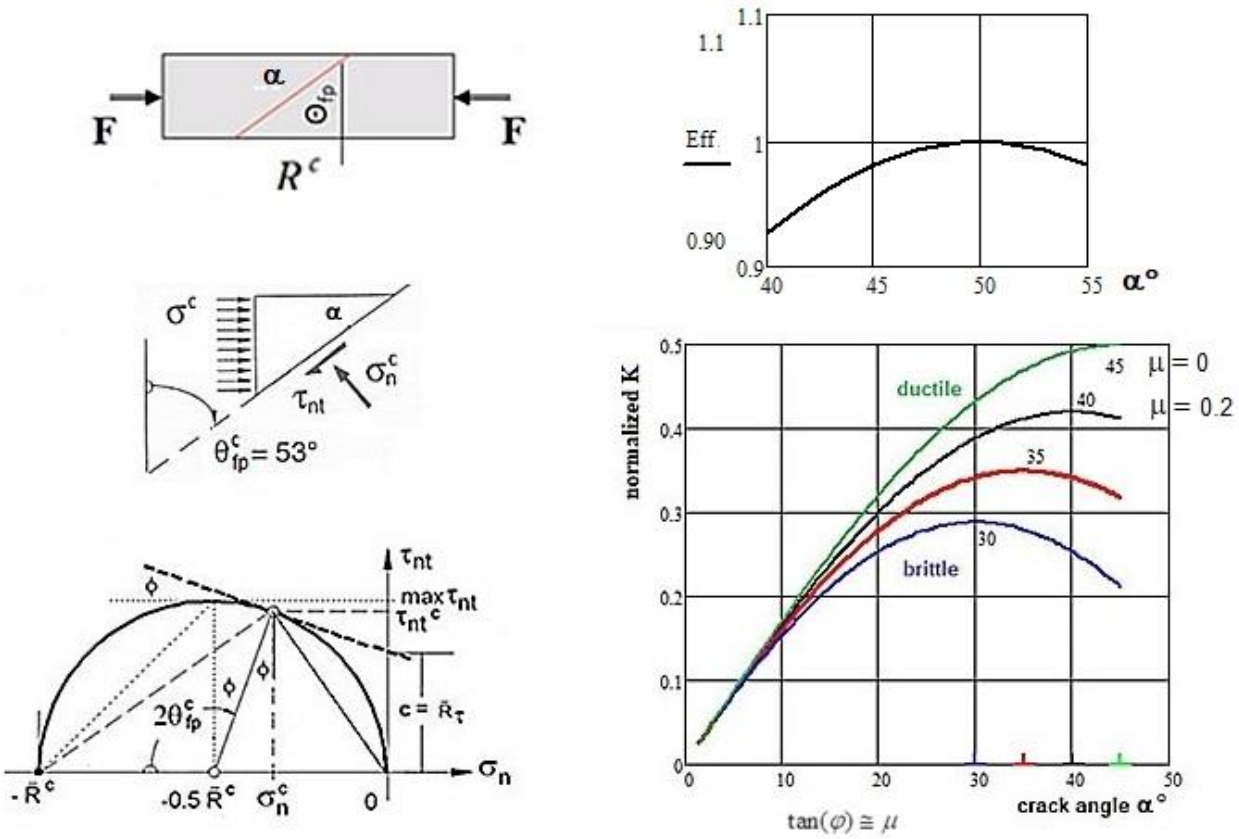

Fig.21: (left) the different angles in strength, Mohr-Coulomb; (right up) dependence of the material stressing effort Eff on the inclination angle α, (right down) K_{IIcr}^c versus inclination crack α considering the friction value μ (here $\Theta_{fp}^c = 90° - \alpha°$ is valid in literature)

LL: A crack α, inclined the same as a compression-induced fracture shear angle Θfp, is linked to minimum energy and to a maximum SIF. Both these values are critical quantities for further crack growth of the solid

6.3 Attempt for an experimental proof under ideal conditions

Of course, more test results are needed for a general proof and validation of the K_{IIcr}^{c} model. And this would be necessary for different brittle materials.

Procedure: One must know the fracture angle $\Theta_{fp}^{c} = 90° - \alpha°$ from the fracture test of the intact test specimen (without crack). Is for instance $\alpha \approx 40°$ then one must laboriously load in this angular range the original crack-free and now in the crack plane laser cut test specimen.

In the tensile case the test specimens with or without a crack are loaded perpendicular to the generated crack or to the still existing crack plane. This should be valid for the compression case, too. Here, two possibilities exist: The compression force (compressive stress) is fixed in its direction and the crack in the test specimen is differently inclined or the crack is spatially fixed and the compression force acts under various angles, *Fig.22*.

From experience with the usual non-cracked compressive strength test specimen is known, that the scatter is high when deriving fracture plane angles Θ_{fp}^{c}. This is caused by the fact that the homogeneity is not ideal. And this non-ideal homogeneity is - from its effect - even more pronounced in the cracked case at the crack tip. Therefore, one assumes an average Θ_{fp}^{c} of about 50° and alters the angle around this value.

Generally there are some standard test set-ups available:

- *The compression test specimens for the envisaged materials are relatively massive. That does not allow the use of a standard Fracture Mechanics test set-up
- *The ARCAN test set-up below for notched test specimens uses inclined butterfly test specimens. ARCAN has the advantage to vary the angle and thus generate bi-axial stress states, *Fig.22*
- *Further, for notched test specimens the Josipescu test set-up is used, however, it allows one inclination angle, only
- *The so-called 'Brazilian splitting test', applied in construction as a thick ring or cylinder [ASTM standard C496], is not appropriate as a possible test set-up. It is a commonly used form of indirect tensions tests in which the specimen is loaded in axial compression, leading to tensile stresses, orthogonal to the applied load, and finally to a guess of the tensile strength.

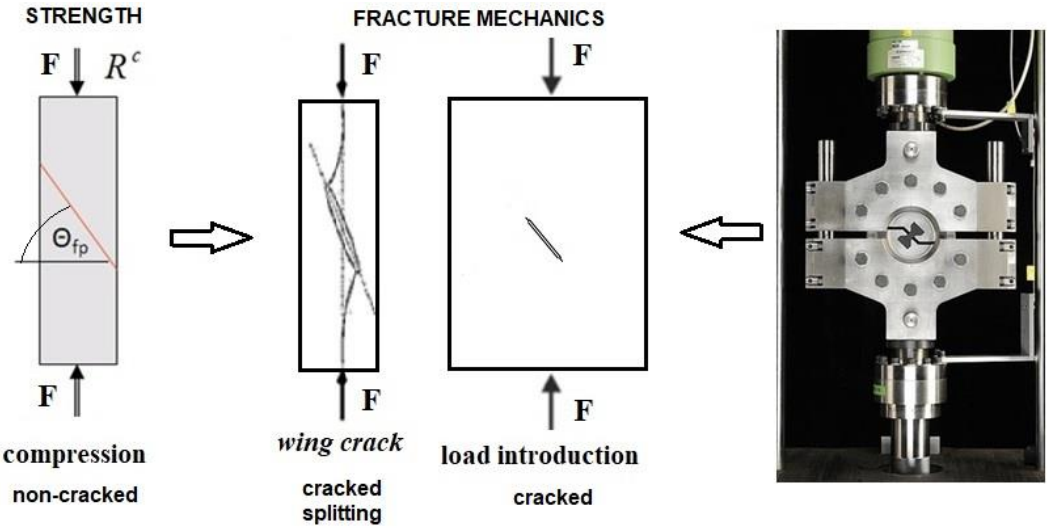

Fig.22: Compression-generated crack in strength mechanics and inclined cracks in fracture mechanics. (right) ARCAN test set-up for 'small' test specimens

Of specific interest, depicted in *Fig.22,* is, that with a non-ideal stress situation at the crack tip, wing cracks will be generated which finally turn into the direction of the compression force.

In *Fig.20* an applicable test set-up is presented. The author uses this test set-up to present in *Fig.23* his idea of the 'Transition from strength mechanics to fracture mechanics'.
The inclined crack represents an initial flaw and is cut under varying inclination angles α to achieve different mixed mode configurations from $K_{Icr}{}^{t}$ (α = 0, $K_{IIcr}{}^{c}$ = 0, experience of splitting danger with wing cracks) to $K_{Icr}{}^{t}$ = 0 for pure shear $K_{IIcr}{}^{c}$. A wing crack initiation will almost occur under the usually non-ideal conditions of the crack angle and the crack tip situation.
The employment of the so-called fracture process zone, suffix $_{fpz}$, in front of the crack-tip would help to assess the crack-tip situation. It practically depends on the test specimen size and the size of the grains. Their maxima are principally linked to the radius of the fracture process zone. As information, for metals the radius of the fracture process zone is approximately

$$r_{fpz} \approx \frac{1}{2\cdot\pi}\cdot\left(\frac{\bar{K}_{Icr}^{\ t}}{\bar{R}^{t}}\right), \quad \bar{K}_{Icr}^{\ t} < \bar{K}_{IIcr} \ \text{(average values}\ ^{-}) \ \text{ in N / mm}^{-3/2}.$$

If the process zone is small compared to r_{fpz}, then the failure is brittle and LEFM is applicable. In the absence of plasticity, we may call the failure *quasi-brittle.*
The crack will close under load and with an increasing inclination angle α, the more. If it is closed then friction occurs on the crack surfaces.

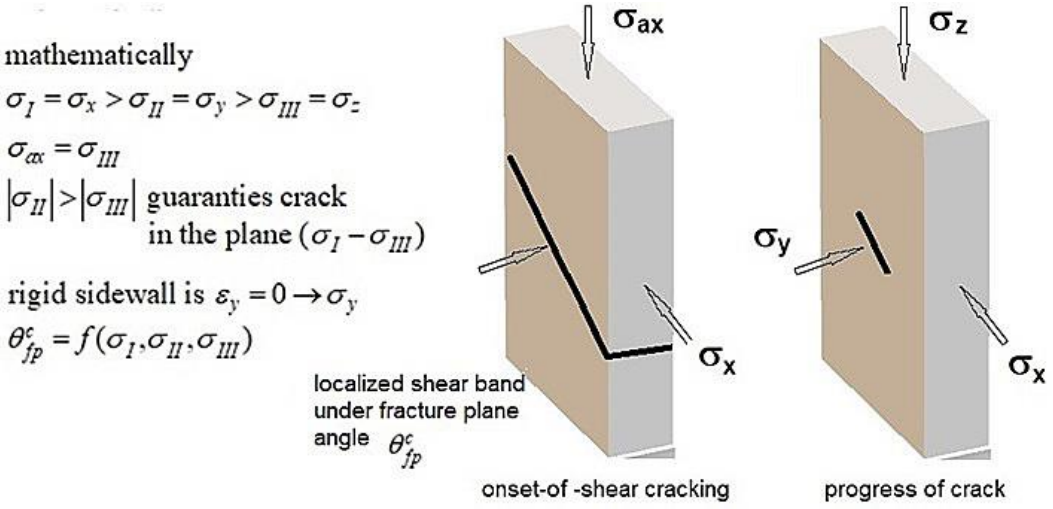

Fig.23: Idea for a test set-up to measure K_{IIcr} . Poisson's ratio-determined plane strain condition, same inclination angle in both the figures

Conclusion and Outlook for isotropic material

- A SFC has to map 3D stress states. It can be validated, principally, by 3D test data sets only. Then, only, the required High-Fidelity is achieved
- If just 2D test data is available, then the 2D-reduced 3D-SFC is applied. This means that the necessary 3D mapping quality is not fully proven
- A test series along a tensile meridian (delivers R^{t}, R^{cc}) or along a compressive meridian (delivers R^{c}, R^{tt}) alone is not sufficient
- For a general 3D-mapping multi-axial failure stress states (R^{tt} , R^{cc}) are required which generate twofold failure modes. Then the significant inherent 120°-symmetry of brittle isotropic materials can be mapped.

Intension of this investigation was to demonstrate, as far as test data was available, that material symmetry might be a sound basis for obtaining a 'closed' building in mechanics desired by the author since about 30 years.
The following results can be now provided supporting the existence of a generic number 2:

- Following Beltrami's statement: The demonstration of an advantageous use of the 'physics-based' invariants I_1 and J_2 for the very different materials concrete, PMMA and foam
- Assessment of critical stress states: The formulations of invariant-based isotropic strength failure conditions (criteria) SFC just need 2 invariants. Due to the fact that a stress state may activate a multi-fold fracture failure type NF or SF the original rotational symmetric fracture body becomes 120°-symmetric. This is tackled by employing the invariant J_3.
- Failure type Normal Yielding NY: It could be shown that this 2nd yield type exists in parallel to Shear Yielding SY. Considering the concave failure surface Drucker's stability postulate is to discuss
- Existence of SIF $K_{IIcr}^{\ c}$: The author also tried to pave the way for a 2nd 'basic' SIF $K_{IIcr}^{\ c}$ in parallel to $K_{Icr}^{\ t} \equiv K_{Ic}$, where the self-explaining suffix $_{cr}$ must (unfortunately) replace the classical $_c$ and where ^{t} denotes tensile and ^{c} compression in order to not confuse readers with two c as indices. The term 'basic' is given to $K_{Icr}^{\ t}$ and $K_{IIcr}^{\ c}$ because the original fracture stress state-induced flaw inclination angle remains stable under further loading and no turning crack under tension or a wing (secondary) crack under compression is activated. The SIF K_{IIcr} and K_{IIIcr} are necessary (friction-free crack surface) for crack-turning Mixed Mode Fracture investigations. The basic SIFs $K_{Icr}^{\ t}$ and $K_{IIcr}^{\ c}$ show equilibrium.

→ Material symmetry seems to have told the author:

In the case of isotropic materials, for the quantities a generic (basic) number of 2 is inherent. This is valid for modes, invariants, yield strengths, fracture strengths, fracture mechanical SIFs and more.

Does this not simplify the engineer's situation and lead to a 'closed macro-mechanical building'?

One might think*: "Material macro-mechanics probably possesses a mathematical order".*

Note on necessary future virtual testing:

For economic reasons in future, at any stage of the design development, product decisions must rely more and more on virtual tests based on reliable and robust structural analysis processes attached to realistic computational simulations. Virtual testing creates new responsibility for the engineer to guarantee the required confidence level by building confidence for taking decisions in design verification and product certification. Therefore efficient SFCs are mandatory to reduce failure risk. Physical testing on material level becomes more important to obtain really 3D-validated SFC models that can demonstrate their predictive capability.
Further confidence will be given if a clear and reliable 'Closed macro-mechanics building' is given indicating which verifications must be performed and which provides the needed reliable SFCs.
This was focused in this paper.

Literature

[Arg73] Argo A S: *Physical basis of distortional and dilatational plastic flow in glassy polymers.* J. Macromol. Sci. Phys B8 (1973), 573-596

[Bre79] Breuer H und Stabenow J: *Schädigungskriterien glasiger Polymere im Hinblick auf deren Schlagzähmodifizierung*. Die Angewandte Makromolekulare Chemie 78 (1979), 45-65. SF-shape is SY-shape

[Kaw88] Kawagoe M and Kitagawa M: *On criteria for craze initiation in glassy polymers*. J. of Materials Science 23 (1988), 3927-3932

[Liu14] Liu J, Zhu Z and Wang B: *The fracture characteristic of three collinear cracks under true tri-axial compression.* The scientific World Journal, V 2014, article ID459025, 5 pages zhemingzhu@hotmail.com

[Mathcad 15]: PTC mathematical program

[Mel77] Melville PH: *Fracture mechanics of brittle materials in compression*. Int. J. Frac.13, 532-534 (cited in Liu 14)

[Mur09] Murthy A R, Ch, Palani G S and Iyer N: *State-of-the-art review on fracture analysis of concrete structural components*. Sadhana Vol.34, Part 2, April 2004, 345-367

[Pha03] Phan A V, Napier J A L , Gray L J and Kaplan T: *Stress intensity factor analysis of friction sliding at discontinuity interfaces and junctions*. Computational Mechanics 32 (2003), 392 -400

[Ste73] Sternstein S S and Myers F A: *Yielding of glassy polymers in the second quadrant of principal stress space.* J. Macromol. Sci, Phys. B 8 (1973), 539-571

[Mat75] Matsushige K, Radcliffe S V and Baer E: *The mechanical behavior of polystyrene under pressure*. J. of Material Science 10 (1975), 833-845

https://www.carbon-connected.de/Group/CCeV.Fachinformationen/Dokumente/Documents/Index/10381

Acknowledgement

Valuable support of this non-funded investigation came from:

- Dipl.-Ing.-Bernd Szelinski for regarding plausibility by 'engineering checking' and for support with Mathcad 15 code problems
- Prof. Dr.-Ing. habil. Wilfried Becker for valuable comments, especially for his "*Do not give up with your search*" for NY and the SIF K_{IIcr}^{c}
- Prof. Dr.-Ing. Wolfgang Brocks for our intensive E-mail-performed conversation.

About the author:

Prof. Dr.-Ing. habil. Ralf Cuntze VDI, Civil Structural Engineer and Hobby-Material Modeler.

1970 – 2004, MAN-Technologie, Development of Structures: ARIANE 1-5 launcher family with different components. Cryogenic Tanks, High Pressure Vessels, Heat Exchanger in Solar Towers (GAST Almeria) and Solar Field, Wind Energy Rotors (GROWIAN Ø103 m, WKA 60, AEROMAN), Space Antennas, Automated Transfer Vehicle (Jules Verne) supplying the space station ISS, Crew Rescue Vehicle (CMC application) for ISS, Gasultra-Centrifuges, and more. Civil Engineering applications: Supermarkets, armoring plans, pile foundation, 5th German climbing garden (designed, concreted and bricked).

Author / Co-author of numerous HSB sheets (1972 - 2015) including transfer with translation of the HSB aerospace structural handbook into English. Co-author of ESA/ESTEC- Handbooks and Standards (1980-2010). Co-author and first convenor of the ESA-Stability Handbook. Surveyor/Advisor for BMFT (MATFO), BMBF (LuFo) and German Research Association DFG

(1980-2009). Editor/convenor/co-author of VDI Guideline 2014 ‘Development of Fiber-reinforced Plastic Components, Part 3 Analysis‘.

Against all institutes, as a single non-funded person, became winner of the World-Wide-Failure Exercise-I (2D stress states) on uni-directional composites and top-ranked in WWFE-II (3D-stress states).

Since 2009 head of the Working Groups ‘Engineering’ (in mechanical engineering), since 2011 ‘Design Dimensioning and Verification’ (in construction), and since 2018 ‘Automated Fabrication in construction’ in the Network CU Bau.

The readership shall forgive the author for not being a full specialist in all domains of this investigation. However, this seems to have been the reason why the work has been done. Without looking over the disciplines’ fences above private research work were not performed. It is an outcome of interdisciplinary.

Comment on the ‘novel-looking’ results above:

“Sometimes you have to learn things that you don't understand easily.
When you have captured them, you can see their use.”
[from a student’s exercise book]

Annex

In the future, interdisciplinary is an urgent **must**. The author was confronted during his life with many engineering disciplines. There is no understanding even amongst the construction disciplines, only. Therefore, many years ago the author tried to simplify the practiced designations. The outcome was a helpful self-explaining, much simpler indexing, that could be used by all structural engineering disciplines. Just for the strength properties the table is given below.

He still hopes that his non-funded GLOSSAR *Fachbegriffe für Kompositbauteile / Technical terms for composite parts* [Springer Vieweg, 2019] will improve understanding between mechanical engineers and civil engineers.

	Fracture Strength Properties										
	loading	**tension**			**compression**			**shear**			
	direction or plane	1	2	3	1	2	3	12	23	13	
9	**general orthotropic**	R_1^t	R_2^t	R_3^t	R_1^c	R_2^c	R_3^c	R_{12}	R_{23}	R_{13}	**friction properties**
5	**UD**	$R_{\|\|}^t$ NF	$R_{\perp}^t$ NF	$R_{\perp}^t$ NF	$R_{\|\|}^c$ SF	$R_{\perp}^c$ SF	$R_{\perp}^c$ SF	$R_{\|\perp}$ SF	$R_{\perp\perp}$ NF	$R_{\|\perp}$ SF	$\mu_{\perp\perp}$, $\mu_{\perp\|}$
6	**fabrics**	R_W^t	R_F^t	R_3^t	R_W^c	R_F^c	R_3^c	R_{WF}	R_{F3}	R_{W3}	*Warp = Fill*
9	**fabrics general**	R_W^t	R_F^t	R_3^t	R_W^c	R_F^c	R_3^c	R_{WF}	R_{F3}	R_{W3}	μ_{W3}, μ_{F3}, μ_{WF}
5	**mat**	R^t	R^t	R_3^t	R^c	R^c	R_3^c	R^τ	R^τ	R^τ	*(≡UD material with turned direction)*
2	**isotropic matrix**	R^t SF	R^t SF	R^t SF	*deformation-limited, cylindrical test specimen bulges: What is then R^c ?*			R^τ	R^τ	R^τ	μ
		R^t NF	R^t NF	R^t NF	R^c SF	R^c SF	R^c SF	R^τ NF !	R^τ NF	R^τ NF	μ